ON WATER MASSES OF THE RED SEA

A THESIS

Presented to

The Faculty of the School of Marine Science

The College of William and Mary in Virginia

In Partial Fulfillment

Of the Requirements for the Degree of

Master of Arts

---

by

Mohamed Zaki Moustafa

1983

LIBRARY
of the
VIRGINIA INSTITUTE
of
MARINE SCIENCE

ProQuest Number: 10626450

All rights reserved

INFORMATION TO ALL USERS
The quality of this reproduction is dependent upon the quality of the copy submitted.

In the unlikely event that the author did not send a complete manuscript
and there are missing pages, these will be noted. Also, if material had to be removed,
a note will indicate the deletion.

ProQuest 10626450

Published by ProQuest LLC (2017). Copyright of the Dissertation is held by the Author.

All rights reserved.
This work is protected against unauthorized copying under Title 17, United States Code
Microform Edition © ProQuest LLC.

ProQuest LLC.
789 East Eisenhower Parkway
P.O. Box 1346
Ann Arbor, MI 48106 - 1346

APPROVAL SHEET

This thesis is submitted in partial fulfillment of

the requirements for the Degree of

Master of Arts in Marine Science

Mohamed Zaki

Mohamed Zaki Moustafa

Approved, April 1983

Evon P. Ruzecki, Ph.D.

Christopher S. Welch, Ph.D.

Albert Y. Kuo, Ph.D.

Ching S. Fang, Ph.D.

William D. DuPaul, Ph.D.

TABLE OF CONTENTS

	Page
ACKNOWLEDGEMENTS	iv
LIST OF TABLES	vi
LIST OF FIGURES	vii
ABSTRACT	ix
I. INTRODUCTION	2
Objective	2
Physiography	2
Meteorological Conditions	5
Tides	5
Currents in the Red Sea	6
Evaporation, Precipitation and River Discharge	7
Previous Work that Bears Directly to the Present Study	8
II. METHODS	11
Data Preparation	11
Segmentation	11
Hypsometric Curves	14
Methods of Data Analysis	14
Volumetric Temperature/Salinity Census	16
Water Type Analysis	17
III. RESULTS AND COMMENTS	23
Volumetric Temperature/Salinity Census	23
Water Type Analysis	29
IV. DISCUSSION	43
Water Type Analysis	46
Circulation	49
V. CONCLUSIONS AND RECOMMENDATIONS FOR FUTURE WORK	52
Suggestion for Future Work	56
BIBLIOGRAPHY	58
VITA	60

ACKNOWLEDGEMENTS

The author wishes to express appreciation to his major professor, Dr. Evon P. Ruzecki, for his patient guidance and encouragement during this investigation. Thanks and appreciation are also extended to Dr. Albert Y. Kuo, Dr. Frank Fang, Dr. C. Welch and Dr. W. D. DuPaul for their criticism of the manuscript. The author also wishes to thank the Department of Physical Oceanography of the Virginia Institute of Marine Science for the computer funds they provided. Special thanks go to Dr. John Zeigler and Dr. Bruce Neilson for their encouragement. The author wishes to thank Dr. A. S. Laughton of the Institute of Oceanographic Sciences for providing the Red Sea bathymetric chart. Finally, I am most indebted to Ms. S. M. Crossley for many hours of typing draft and final copies of this manuscript.

DEDICATION

This work is dedicated to my parents, Zaki and Samiah Moustafa who loved, encouraged and cared for me all my entire life.

LIST OF TABLES

TABLE PAGE

1 Volume as a Percent of the Three Main Red Sea Water Masses Identified Seasonally..... 29

LIST OF FIGURES

FIGURE		Page
1.	Bathymetric chart of the Red Sea	3
2a.	Segmentation of the Red Sea and locations of sample stations used in the winter analysis	12
2b.	Segmentation of the Red Sea and locations of sample stations used in the summer analysis	13
3a.	T/S scatter plot for the Red Sea during summer	20
3b.	T/S scatter plot for the Red Sea during winter	21
4.	Volumetric temperature/salinity census of the Red Sea water for summer	24
5.	Volumetric temperature/salinity census of the Red Sea water for winter	25
6.	Detailed volumetric temperature/salinity census of Red Sea water for summer	27
7.	Detailed volumetric temperature/salinity census of Red Sea water for winter	28
8.	Parent types A and C distributions for summer	30
9.	Parent type B distributions for summer	31
10.	Temperature distributions along the central axis of the Red Sea for summer	32
11.	Salinity distributions along the central axis of the Red Sea for summer	34
12.	Parent type D distributions for summer	35
13.	Temperature distributions along the central axis of the Red Sea for winter	37
14.	Salinity distributions along the central axis of the Red Sea for winter	38
15.	Parent type B distributions for winter	39

Figure Page

16. Parent type E distributions for winter..... 40

17. Parent type F distributions for winter..... 42

18. Distributions of parent types A, B, C and D in the Red Sea during summer..... 45

19. Distributions of parent types E, F and B in the Red Sea during winter..... 48

ABSTRACT

A volumetric temperature/salinity analysis was applied to multiannual hydrographic data from the Red Sea for summer and winter periods. The analysis shows three water masses dominate the basin: Red Sea Bottom Water accounts for 57% of the total volume during summer and 53% in winter; Intermediate Water fills 19% of the basin in summer and 28% in winter; and a newly defined water mass, Red Sea Upper Water, fills 5% of the basin in summer and 8% in winter. A water type analysis was applied to the data to determine the origin of each water mass and shows Red Sea Bottom Water with T/S values of 21.5°C and 40.5°/oo is formed during winter as a mixture of water types originating in the Gulf of Suez and the northern section of the Red Sea (28°N). The upper water mass results from mixing of water types formed during summer in the Gulf of Suez, at intermediate depths in the Gulf of Aden and at the surface in the Red Sea near 13°N. Red Sea Intermediate Water results from mixing of the surface and bottom water masses.

Winter flushing of the Gulf of Suez and subsequent mixing is sufficient to renew Red Sea Bottom Water in a time scale of 10 to 20 years which is also in agreement with estimates by other authors. Loss of bottom water to the Gulf of Aden over the sill at the straits of Bab el Mandeb occurs during winter with the exiting of Red Sea Intermediate Water at the bottom. Seasonal configurations of isopleths of equal concentration of the various water types as well as isotherm configurations suggest a seasonal reversal of two layer flow over the sill with surface inflow and bottom outflow during winter and opposite flows during summer. These exchanges are attributed to thermohaline circulation of deeper waters and the monsoon dominated wind driven surface circulation and explain the summer increase in volume of Red Sea Bottom Water which is formed during winter.

ON WATER MASSES OF THE RED SEA

I. INTRODUCTION

Objective

The objective of this investigation is to formulate seasonal volumetric temperature salinity censuses for meridional segments of the Red Sea through analysis of available data and to identify predominant and secondary water masses from each census. Censuses are compared to determine seasonal changes and the extent of exchange of water with the Arabian Sea through the Strait of Bab el Mandeb. Finally, the question of the origin of the Red Sea water masses is addressed: Are water masses formed in the Red Sea or are they the result of advection?

Physiography

The Red Sea

The Red Sea is a flooded rift valley that can be described as a young ocean which is being formed by the pulling apart of Arabia and Africa. From the Strait of Bab el Mandeb in the south to the Sinai Peninsula in the north, it is approximately 1850 km long with an average width of 220 km. At the Strait of Bab el Mandeb it narrows to 27 km wide (at Perim Island) and has a sill depth of 100 m. This shallow sill, separating the Gulf of Aden and the Red Sea, is located near the Hanish Islands, 125 km north northwest of Perim Island. Bathymetry of the southern Red Sea is characterized by a wide shelf containing shallow reefs and many small islands (Fig. 1). In the

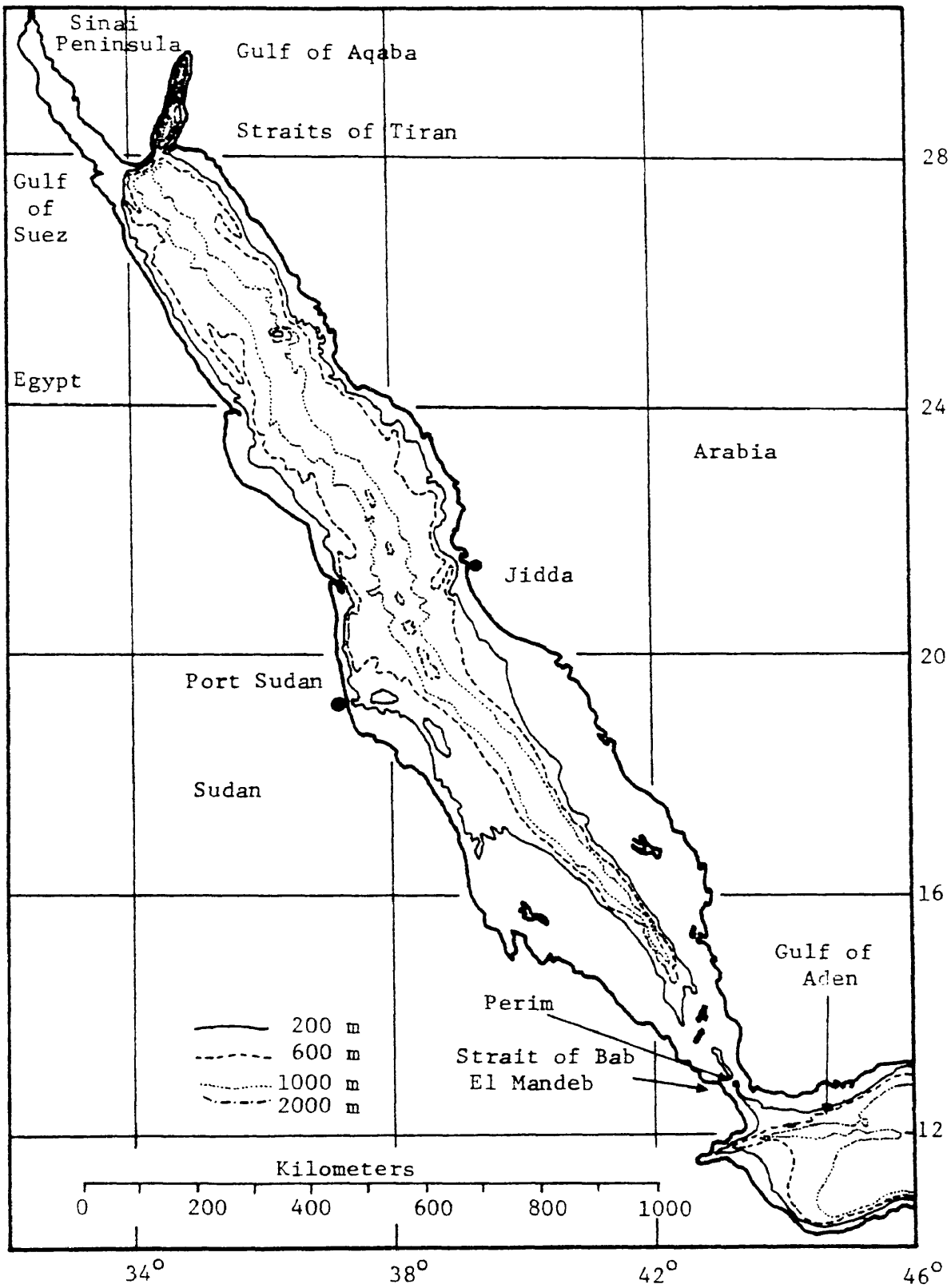

Figure 1 . Bathymetric chart of the Red Sea.

north, coastal shelves are narrower, and mean cross-sectional depths are much greater than in the south. Near 28°N the Red Sea branches into the Gulf of Suez and the Gulf of Aqaba. Although similar in shape and surface area they differ in that the Gulf of Suez has a mean depth of only 40 m while the Gulf of Aqaba is a deep rift basin (Neumann and McGill, 1961).

The Gulf of Aqaba

The Gulf of Aqaba is part of the Syrian-African rift system. It is 170 km long, 14-26 km wide, more than 1800 meters deep and is separated from the Red Sea by a 252 meter deep sill at the Straits of Tiran. Its shelves are narrow and its shores and submarine slopes extremely steep. The climate of the area is arid and hot, prevailing winds are from the north, and evaporation is high, especially in winter. The rather uniformly highly saline waters are warm throughout the year. Temperatures are consistently above 22° in winter (Neumann and McGill, 1961).

The Gulf of Suez

In contrast to the Gulf of Aqaba, the Gulf of Suez is very shallow with an average depth of 40 meters and no sill at its juncture with the Red Sea. The climate is very much like Aqaba and the northern part of the Red Sea. Water characteristics in the Gulf of Suez are strongly influenced by the local climate which results in temperature and salinity values of 18.0 to 18.5°C and 41.5°/oo in winter and 25.0 to 26.0°C and 41.8 to 42.0°/oo in summer.

The Gulf of Aden

The Gulf of Aden occupies the northwestern part of the Arabian Sea. A 125 meter deep sill, located near Hanish Island, results in

limited exchange of water with the Red Sea. Depths over 3000 meters occur in several places near the center of this Gulf.

Meteorological Conditions

High mountains and high plateaus on both sides of the Red Sea constrain the monthly mean atmospheric circulation in the lower troposphere to flow parallel to the sea axis. However near the coasts, wind alternate daily between a nocturnal land breeze and a daytime sea breeze. This well developed, daily pattern is caused by large diurnal differences in local heating (Flohn, 1969). Monthly mean surface wind vectors for 1° squares in the Red Sea and the Gulf of Aden show that winds are directed primarily both north and south along the central axis of the Red Sea, with only slight variations in speed and direction (K.N.M.I., 1949). Throughout the year, winds north of 19°N in the Red Sea, are from the north-northwest while south of this latitude they are controlled by the monsoon system and reverse direction twice annually. During the southwest monsoons (June to September) winds in this southern portion are from the north to north-northwest while during northeast monsoons (October to May) they blow from the southeast to south-southeast. The weak north-northwest winds in the north ($\sim$ 2.4-4.4 ms^{-1}) and the strong south-southeast winds in the south ($\sim$ 6.7-9.3 ms^{-1}) converge near 19°N. This convergence zone gradually moves southward until by June the winds are from the north-northwest for the entire length of the Red Sea (Patzert, 1972).

Tides

Red Sea tides are predominantly semidiurnal. Tidal motion in the Red Sea is a result of two, almost equal, generating forces:

astronomical tides generated within the Red Sea and the co-oscillating tide from the Gulf of Aden (Defant, 1961). Tides oscillate in such a way that north of the nodal point (19.5°N) the tide will be high when the tide is low to the south. The amplitude of this oscillation is approximately 0.7 m in the north and 1.0 m in the south. Bibik (1971) states that the velocity of tidal currents of the main lunar semidiurnal wave are equal to 2-5 cm s^{-1} in the southern part of the sea, 6 cm s^{-1} in the central region, and 2 cm s^{-1} in the north.

Currents in the Red Sea

Summer

During the southwest monsoons (June to September), winds and mean surface currents are directed toward the Gulf of Aden. These north-northwest winds and south-southeast currents pass through the Strait of Bab el Mandeb to join the strong atmospheric and oceanic flow directed from the Gulf of Aden into the Arabian Sea. During late summer, speeds of the south-southeast flowing current north of 26°N increase, apparently due to the strong north-northwest winds present at this time. Although the winds are weak over the southern Red Sea during July and August, strong southerly currents are present in the central portion between 18° and 20°N. The strongest flow occurs during July in the Strait of Bab el Mandeb, when speeds of over 20 cm s^{-1} are calculated for the surface outflow (Patzert, 1972).

Winter

During the northeast monsoon season in the Indian Ocean (October through May), winds of the Gulf of Aden shift to south-southeasterly and increase in strength as they enter the Strait of

Bab el Mandeb. Surface waters of the Gulf of Aden are driven into the Red Sea and flow northward. Direct surface current measurements made during November and March in the Strait of Bab el Mandeb (Siedler, 1968) show mean inflow of 60-80 cm s^{-1}. In the northern half of the Red Sea, the wind blows from the north northwest resulting in a southerly flow. Between 24° and 27°N a cyclonic eddy is found during this season Boisvert, (1966).

Transition Periods

During periods when monsoon winds of the southern Red Sea change direction (May through June and September through October), monthly mean currents are weakest and most variable. In the southern Red Sea during early June, the currents change direction approximately in phase with the shift in wind direction from the south southeast to the north northwest (Patzert, 1972). In the central Red Sea, as these south southeast winds decrease in strength, the current reverses and begins to flow southward. To the south, with the onset of the northeast monsoon or south southeast winds in early September the change in current direction lags behind the change in wind direction by approximately one month.

Evaporation, Precipitation and River Discharge

Because rainfall is slight and no large rivers discharge into the Red Sea, the diluting effects of precipitation and runoff are negligible (Thompson, 1939a). The exchange between the Red Sea and the Suez Canal, to the north, when compared to the flow through the Strait of Bab el Mandeb, to the south, is also insignificant (Siedler, 1969), hence, the loss of water due to large excess of evaporation

over precipitation for the entire Red Sea is balanced by an inflow of water from the Gulf of Aden.

Estimates of average evaporation vary from 183 cm yr^{-1} by Privett (1959) to 230 cm yr^{-1} by Yegorov (1950). Privett's results are believed to be an improvement over the earlier estimate (Morcos, 1970) and show that maximum evaporation occurs during January in the northern Red Sea and during November in the southern Red Sea. These evaporation maxima result from strong winter winds in the south and large winter vapor pressure gradients over the sea surface in the north (Privett, 1959).

Previous Work that Bears Directly to the Present Study

The most striking feature of the hydrographic structure of the Red Sea is high salinity. Surface salinities vary from 37.0^{o}/oo at the southern entrance near the Strait of Bab el Mandeb to more than 40.0^{o}/oo in the north. Because of these high salinities and the arid climate of the area, many investigators concluded that evaporative processes control the surface circulation (Neumann and McGill, 1961; Siedler, 1969; Everett and Browning, 1971). However, earlier investigators viewed the situation somewhat differently, and recognized that the winds exert a strong influence on the circulation (Thompson, 1939b, and Barlow, 1934). Neither group, however, mentioned the water masses of the Red Sea or identified their region of formation. Such information would provide evidence for temporal and spatial variation in the thermohaline circulation. In his volumetric statistical T/S analysis of the Arabian and Red Sea water masses, Dubrovin (1964) used observations from ten Red Sea stations obtained in June, 1958. He

concluded that extreme uniformity is a feature of the Red Sea water masses, with 75% of the volume included in a single T/S class (21.0-22.0°V, 40.5-41.0‰). His data, however, was limited to one set, in June 1958 and his T/S class size was 1°C by 0.5‰. Privett (1959), concluded that cooling and evaporation in the Red Sea are greatest in winter and result in surface temperature depression of 2°C. Although salinity varies from 37‰ near Bab el Mandeb to more than 40.0‰ in the northern part of the Red Sea, there are no large seasonal changes in average salinity (Siedler, 1968). Minimal vertical gradients of both temperature and salinity in the surface layer in the northern part and maximum evaporation and cooling during winter prompted, Neumann and McGill (1961) to suggest that deep water (21.0 to 22.0°C and 40.5 to 41.0‰) may be formed in the northern part of the Red Sea at that time. Results of these investigations suggest the following questions pertaining to the Red Sea water masses:

1. Are the seasonal volumetric temperature-salinity censuses of water masses in the Red Sea similar?

2. What is the origin of the Red Sea bottom water and other water masses?

   (A similar question was raised by Patzert (1972))

3. Are the water masses in the Red Sea formed locally or are they the result of advection?

This investigation answers these questions by analysis of historical Red Sea hydrographic data collected in the Red Sea from 1958 to 1966 and obtained from the National Oceanographic Data Center (NODC).

The results of this investigation are presented as a series of chapters, which in turn, are divided into section. Chapter II describes the methods of the analytical techniques used to obtain the results. The results of the analysis are presented, with comments, as Chapter III and the final chapter interprets these results, ending with conclusions based on this study and suggestions for further investigation.

II. METHODS

Data Preparation

Hydrographic data taken in the Red Sea prior to 1966 was obtained from NODC and includes 721 stations where temperature or salinity measurements were made at standard depths. Data from several of these stations were not used in this study for two reasons: many were in shallow water (less than 30 meters), and stations prior to 1948 did not have paired temperature and salinity observations. For the analysis, all available hydrographic stations occupied between 1958 and 1966 were used for the two main seasons. These seasons are easily delineated in the Red Sea by the monsoon character of prevailing winds: winter (December through March) and summer (June through September). The total number of stations used was 157: 71 occupied in winter and 86 in summer at locations shown in Figures 2a and b. Because potential temperature of a sample is not a function of the sample depth, it is a more useful parameter than *in situ* temperature for tracing water masses in the ocean. Therefore, *in situ* temperature was converted to potential temperature (Rosenblum, 1980) and σ_θ calculated. Although data describing the hydrographic structure are not available for all areas in the Red Sea, those that are were sufficient to allow consideration of seasonal mean longitudinal structure.

Segmentation

For the purpose of this study, the Red Sea was initially divided into ten segments of equal length (200 km) along its

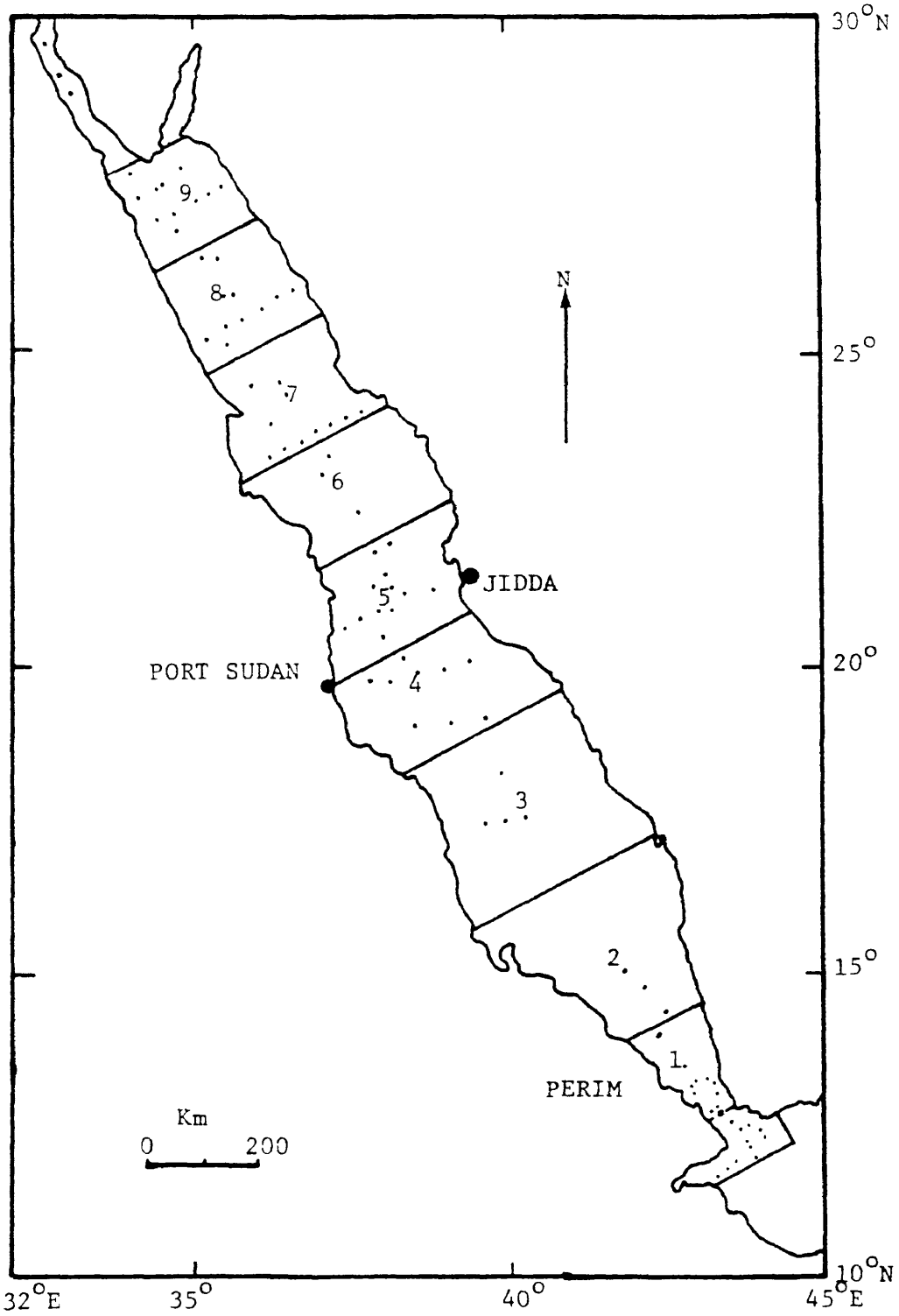

Figure 2-a . Segmentation of the Red Sea and locations of sample stations used in the winter analysis.

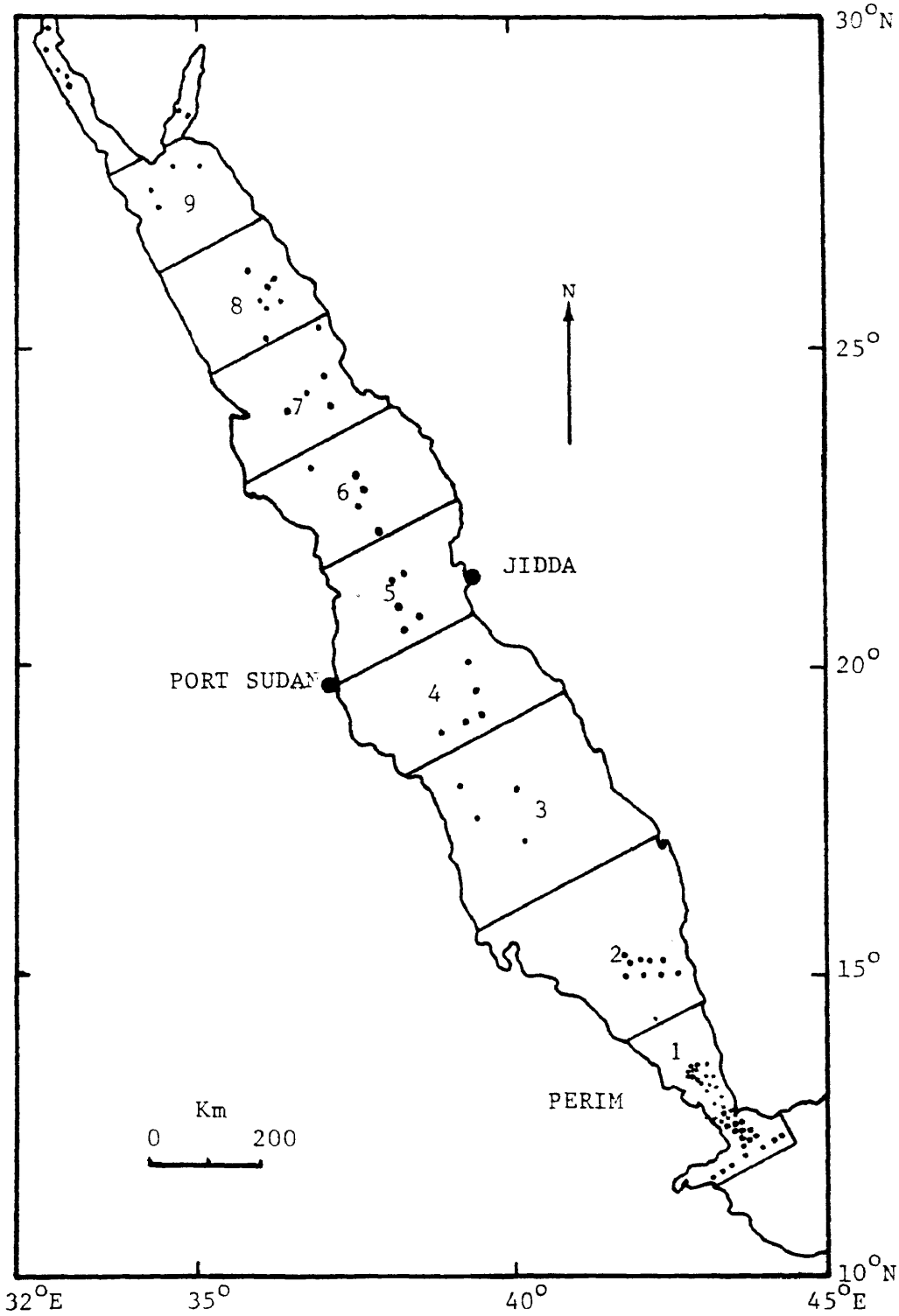

Figure 2-b. Segmentation of the Red Sea and locations of sample stations used in the summer analysis.

LIBRARY
of the
VIRGINIA INSTITUTE
of
MARINE SCIENCE

longitudinal axis. Non-uniform spacing of historical stations in both seasons required adjustment of segment length in the southern region. Final partitioning resulted in nine segments shown in Figures 2a and b. The first segment (1) encompasses the sill region and Hanish Island, and an exterior segment represents the Gulf of Aden. The northernmost segment (9) terminates short of the Gulfs of Suez and Aqaba allowing independent treatment of these embayments. Segmentation was performed on a recently prepared bathymetric chart of the Red Sea (Laughton, personal communication) Mercator projection (Figure 1).

Hypsometric Curves

Hypsometric curves were prepared for the ten segments used (Aden and 1 through 9) and the Gulfs of Suez and Aqaba. For each segment, areas between successive isobaths were measured with a digital planimeter. The planimeter scale reading was multiplied by a scaling factor determined by planimetering a 100 x 100 km^2 area at mid latitude (20^oN) in the Red Sea chart. Surface area measured in each segment was then adjusted to the area measured at 20^oN (Eugene, 1966). The total Red Sea surface area was found to be $4.9 \times 10^{11} m^2$.

Methods of Data Analysis

Potential Temperature, Salinity Plots

Potential temperature and salinity data were averaged in each segment (1 through 9) and both Gulfs for all nine years, for each season, and thus, were reduced to a single curve (θ vs. depth and S vs. depth) representing a segment. Standard error for every averaged value, at standard depth, was then calculated employing the method described by Sokal and Rohlf (1969). Assuming linear changes of θ

and S between measurements, the depths of 0.1°C isotherms and 0.1‰ isohalines were determined for each segment/season combination.

Rationale for Averaging Data Within Each Segment

Recently published discussions of the transverse structure of the Red Sea suggest that lateral variations are transient and can be ignored when considering the mean seasonal structure. For example, during the ATLANTIS Red Sea expedition of June 1958, two transverse sections were occupied. Neumann and McGill (1961) concluded that the resulting data showed no obvious lateral gradients at the surface or at depth. Maillard (1971) analyzed the lateral and longitudinal hydrographic structure of the Red Sea during February 1963, based on a geostrophic interpretation of hydrographic data and G.E.K. observations made aboard R/V COM. R. GIRAUD during January-February, 1963. She hypothesized that the circulation at that time consisted of a series of large eddies, causing strong cross-currents. She concluded, however, that more observation were needed before the complexities of the Red Sea circulation could be understood. Perhaps the large variations in hydrographic structure that she interpreted as eddies and strong currents were only transient, and were induced by strong tidal currents that are known to perturb the mean structure (Patzert, 1972). Robinson (unpublished manuscript) described the mean monthly variations in the lateral temperature structure of the Red Sea using bathythermograph data. Patzert (1972), using the same data set, concluded that the data were inadequate to determine any lateral temperature variations.

Monthly mean meteorological surface data show that there are little lateral variations in wind and atmospheric pressure across the Red Sea (KMNI, 1949), hence, large lateral variations in the hydrographic structure should not be expected.

As part of the present investigation, the previously mentioned ATLANTIS transverse sections were examined to determine the extent of vertical variations between successive 0.1°C isotherms and 0.1°/oo isohalines. The examination showed that the thickness of any layer varied by only 2 to 3% along the length of a transect (200 km) thus indicating no large lateral variation in the hydrographic structure perpendicular to the longitudinal axis. The largest variation (± 17%) of layer thickness was found in maximum gradient regions, which was expected. However, because the layer thickness in maximum gradient regions is less than 0.5 meters, the volumes represented are insignificant compared to those of the mixed layer or bottom water. Thus, one can conclude that an accurate first order approximation of the longitudinal hydrographic structure of the Red Sea can be obtained by using averaged temperature and salinity values for each segment.

Volumetric Temperature/Salinity Census

A temperature salinity thickness census was prepared for each segment. Methods of preparation were similar to those described by Wright and Parker (1976). Temperature and salinity class sizes were set at 0.1°C and 0.1°/oo . The technique was as follows:

The depth of each 0.1° isotherm and each 0.1°/oo isohaline was determined from processed station data by linear interpolation between standard depth intervals. Depths were arranged in increasing order with the associated isotherm or isohaline values. The thickness of each layer bounded by either successive isotherm-isohaline, isotherm-isotherm or isohaline-isohaline pairs was determined by taking the difference between successive depths (in meters). The thickness of each layer then was multiplied by unit area, obtained

from the hypsometric curve, to arrive at the volume for each T/S class in a segment. Finally, summer and winter individual volumetric temperature salinity censuses were summed to yield two volumetric temperature salinity censuses for the entire Red Sea.

Water Type Analysis

Mixing of two water types may be illustrated on a T/S diagram by a straight line drawn between their two representative points. The proportionate distance to any point along the line from one water type is inversely proportional to the percent of that water type in the mixture (Sverdrup, et al., 1942).

Given three water types of differing temperature and salinities, an infinite number of mixtures may be obtained with each mixture falling within the confines of a triangle delineated in T/S space by the three original water types. Conversely, given a parcel of water with known temperature and salinity and three parent water types, the percent of each parent water type required to produce the temperature and salinity of the parcel can be specifically determined by any of several numerical or geometric methods (for details, see Ruzecki, 1979).

Temperature salinity correlation plots for each season were used to determine the location, in T/S space, of four parent types which, when mixed in varying proportions, would yield all possible T/S pairs encountered during a season. Three criteria were used as guides to determine the selection of parent water types:

- they were to conform, when possible, to water types established in the literature;

o their positions in temperature-salinity space must be such that they form the smallest trapezoid encompassing all T/S values encountered during a particular season;

o they were to vary as little as possible from one season to the other.

The four parent water types selected were

A. Gulf of Aden intermediate summer water (temperature = 18.0°C, salinity = 35.0‰).

B. Gulf of Suez winter water (temperature = 18.0°C, salinity = 41.5‰).

C. Gulf of Suez summer water (temperature = 27.0°C, salinity = 41.8‰).

D. Red Sea surface summer water from the southern region (temperature = 33.0°C, salinity = 37.2‰).

These parent water types were treated as contributing sources for the summer. Two new parent water types were used as contributing sources during winter; but, in themselves, are a mixture of two basic parent water types:

E. Temperature = 28.9°C, salinity = 40.3‰, a mixture of 73% Suez summer parent water type (C above) and 27% Red Sea surface summer water (D above).

F. Aden surface water temperature = 25.8°C, salinity = 36.2‰, a mixture of 53% Red Sea summer water (D above) and 47% Aden intermediate water (A above).

The exact T/S positions of parent water types used for a particular season were plotted to be the corners of a trapezoid for summer and a triangle for winter. Parent waters are plotted on a T/S plane as circled dots in Figures 3a and 3b.

To investigate the longitudinal relationships of surface salinities, a multiple regression model was constructed with Gulf of Aden or Suez surface salinities of the upper 200 meters as the dependent variable and the Red Sea surface salinities the independent variable. The results showed that:

o surface salinities in segments 1 and 2 are strongly related to Gulf of Aden surface salinities. The relationship is not as strong for the other segments.

o surface salinities in segments 3 through 9 are well related, not to Gulf of Aden, but to Gulf of Suez however; the relationship is not as high as for segments 1 and 2.

Summer Parent Water Types

During the summer season a parcel of water, in the upper 200 m, of segments 1 and 2 is apparently formed by a mixture of parent water types, A, B and D rather than B, C and D. On the other hand, a parcel found in segments 5 through 9 is a mixture of parent water types B, C and D rather than A, B and D. All water deeper than 200 m is formed by mixing of parent water types B, C and D in the whole region (see Figure 3-a).

Winter Parent Water Types

In contrast to summer, all winter T/S values fall within one triangle delineated by B, E and F parent water types where E is a mixture of D and C and F is a mixture of A and D as described above (see Figure 3-b).

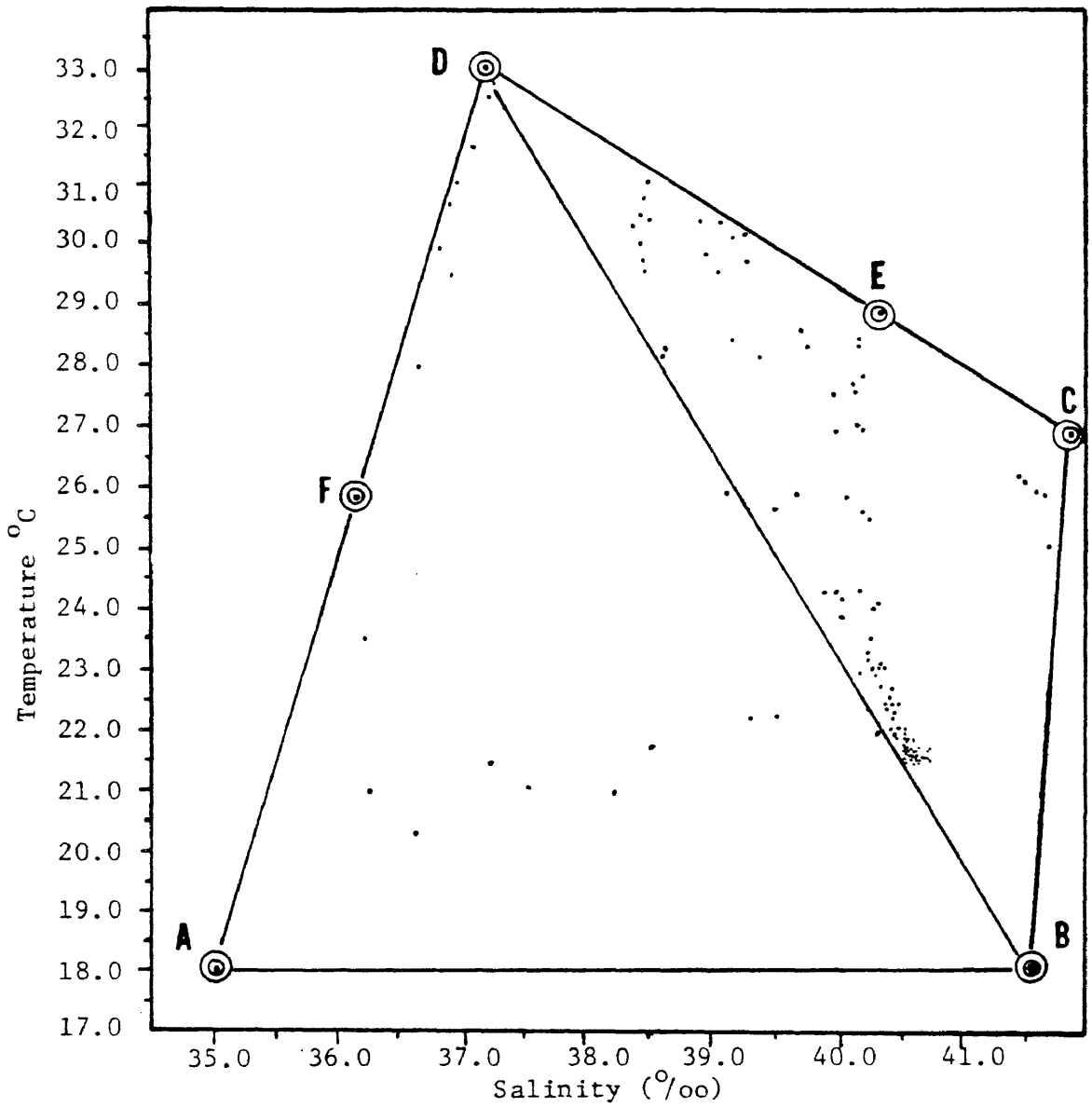

Figure 3-a . T/S scatter plot for the Red Sea during summer. Circled dates indicate T/S values of parent water types used in the analysis. (see text for names and T/S values of each water type).

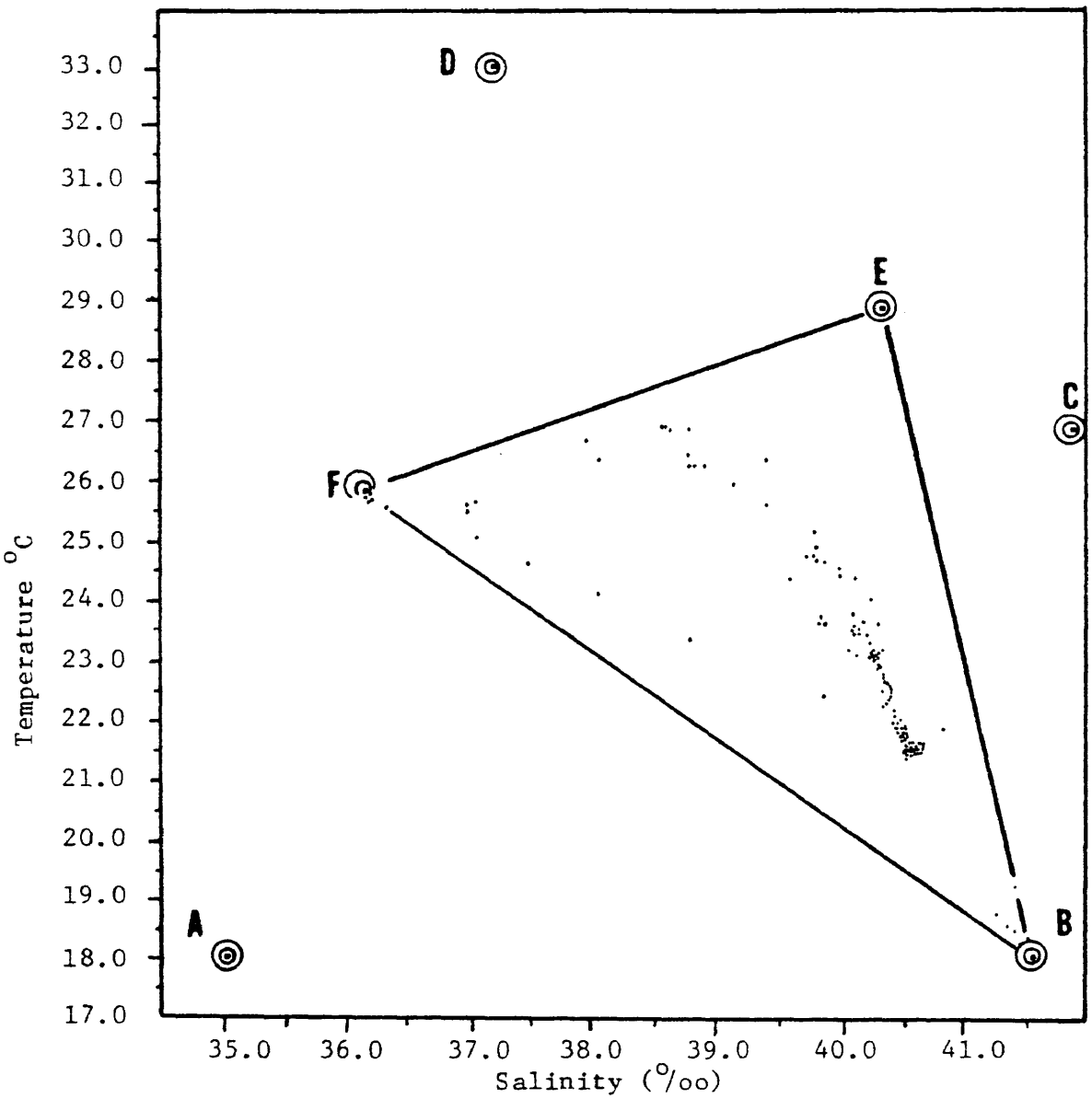

Figure 3-b. T/S scatter plot for the Red Sea during winter. Circled dates indicate T/S values of parent water types used in the analysis. (see text for names and T/S values of each water type).

With these criteria, the percent of each parent water type were calculated for all averaged T/S pairs in each segment. Plots showing percent water types as functions of axial position and depth are truncated by 500 meters because below this depth all the water is attributable to Red Sea Bottom Water.

III. RESULTS AND COMMENTS

Qualitative results of the data analysis are presented as the distribution of potential temperature, salinity and sigma θ. Quantitative results are presented as volumetric temperature salinity censuses.

Volumetric T/S Census

A quantitative analysis was assisted by casting the data in array form representing a volumetric T/S census. A single census for the study area was formulated to establish the importance and interrelationships of the various water masses encountered. Summing all individual censuses for a season resulted in two censuses for the Red Sea. These were used to identify water masses found in the Red Sea by employing the method described by Wright and Parker (1976) with individual T/S classes of each census ranked according to volume. Temperature/salinity class size was selected at 0.1^{o} and $0.1^{o}/oo$ and the resulting censuses are shown in Figures 4 and 5. Numbers in each class denote volume in km^3. Total volume of the Red Sea was found to be 170817 $km^3 \pm 1.9\%$. The variation is attributed to round off and smoothing errors inherent in the methods used to prepare the censuses.

Summer

From a T/S census one can determine the largest classes, by volume, as well as define the limits of dominant water masses. The

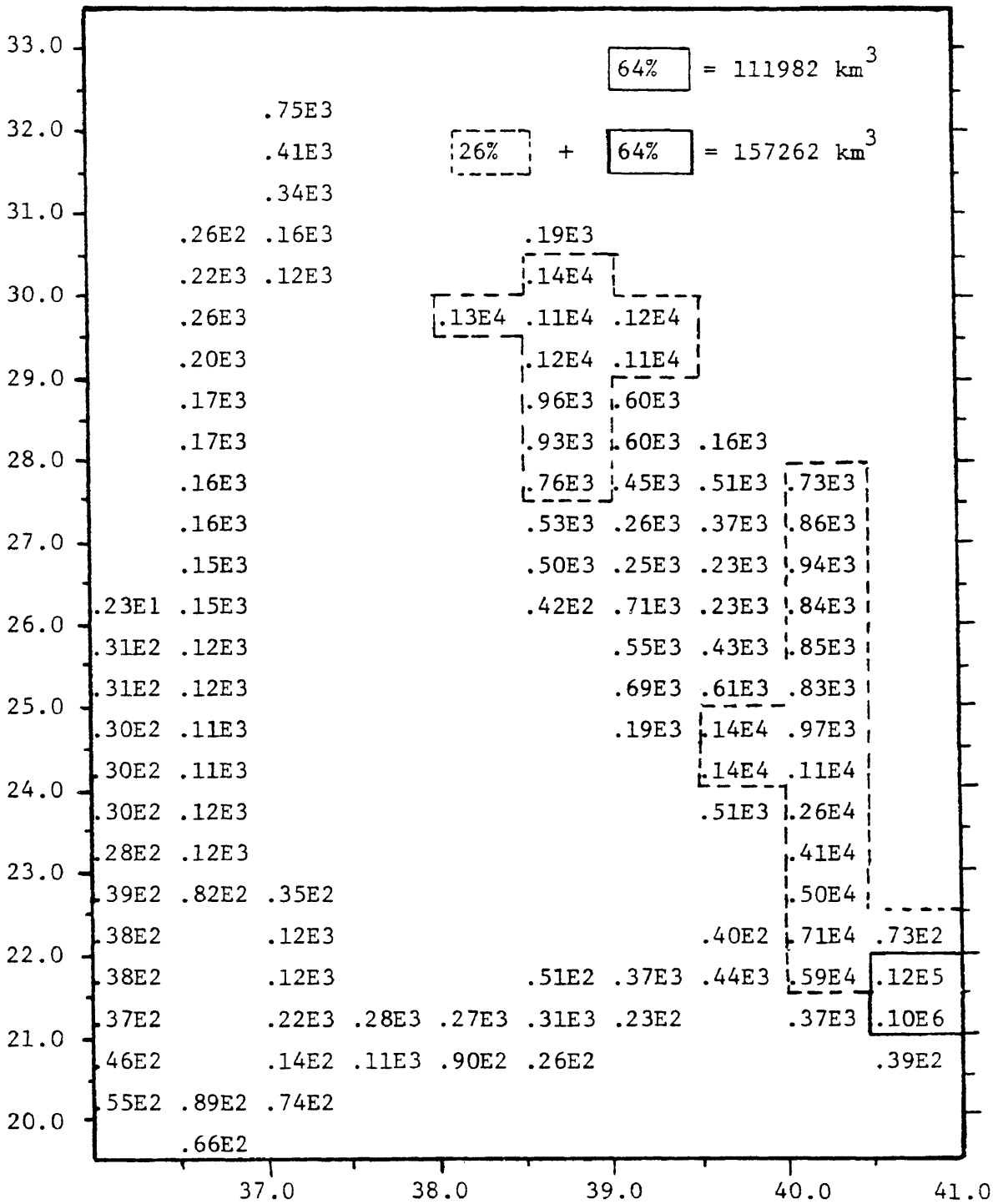

Figure 4. Volumetric temperature/salinity census of the Red Sea water for summer. Values are in km^3. Classes are bounded by 0.5°C and 0.5 ‰ . (.12E5 = $0.12 \times 10^5 km^3$)

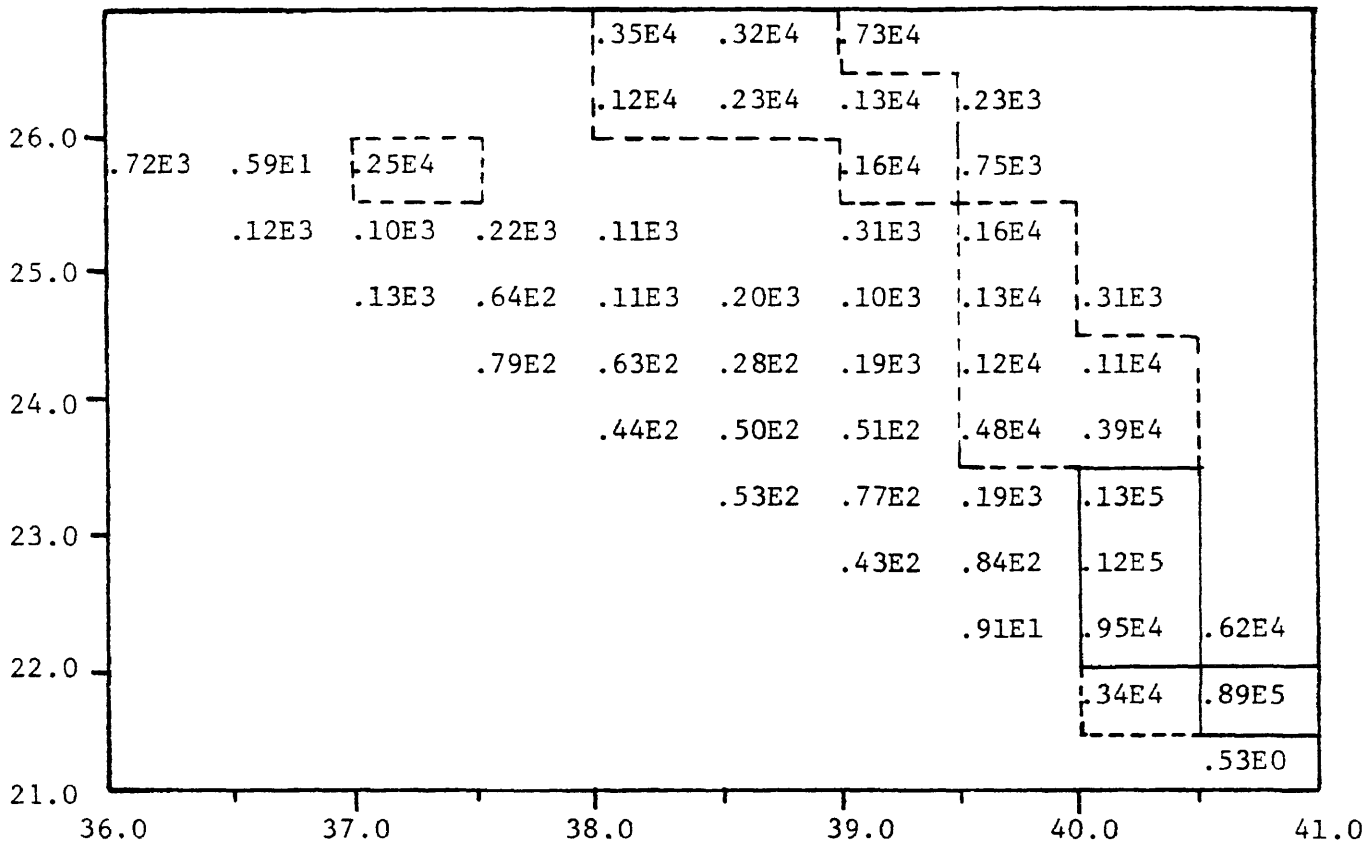

Figure 5. Volumetric temperature/salinity census of the Red Sea water for winter. Values are in km^3. Classes are bounded by 0.5°C and 0.5 ‰.

73% = 123431 km^3

73.7% + 17.6% = 152907 km^3

largest T/S class encountered during summer accounts for 57.4% of the water volume in the Red Sea. It represents the Red Sea bottom water with temperature and salinity of 21.6 and 40.6$^{o}/oo$ (Neumann and McGill 1961) which puts it in Dubrovin's (1964) T/S class of 21.0 to 22.0 and 40.5 to 41.0$^{o}/oo$. An expanded and detailed portion of the summer census, Figure 6, shows Red Sea bottom water can be further identified by water in the ten T/S classes bounded by 21.5-22.0^{o}C and 40.5-40.8$^{o}/oo$.

The second largest mode accounts for 18.5% of the total volume in summer. It falls in classes bounded by 22.0-24.0^{o} and 39.9-40.5$^{o}/oo$ and is defined as Red Sea Intermediate Water. This water mass, was not reported by Dubrovin (1964) in his Red Sea volumetric T/S census for June.

The third largest mode found during summer is given the name "Upper Water Mass". It accounts for 5.1% of the total volume and is bounded by 24.0-31.0^{o}C and 38.4-40.3$^{o}/oo$. During this season the upper water mass is confined to the upper 100 m of the water column. Red Sea Intermediate Water occupies the region between 100 and 200 m and Red Sea Bottom Water fills the basin below 200 m.

Winter

According to Neumann and McGill (1961) bottom water may be formed in the Red Sea during winter because evaporation and cooling are at their maxima. An expanded and detailed portion of the winter census, Figure 7, shows the opposite. Red Sea Bottom Water accounts for 53.3% of the total volume during this season. Red Sea Intermediate

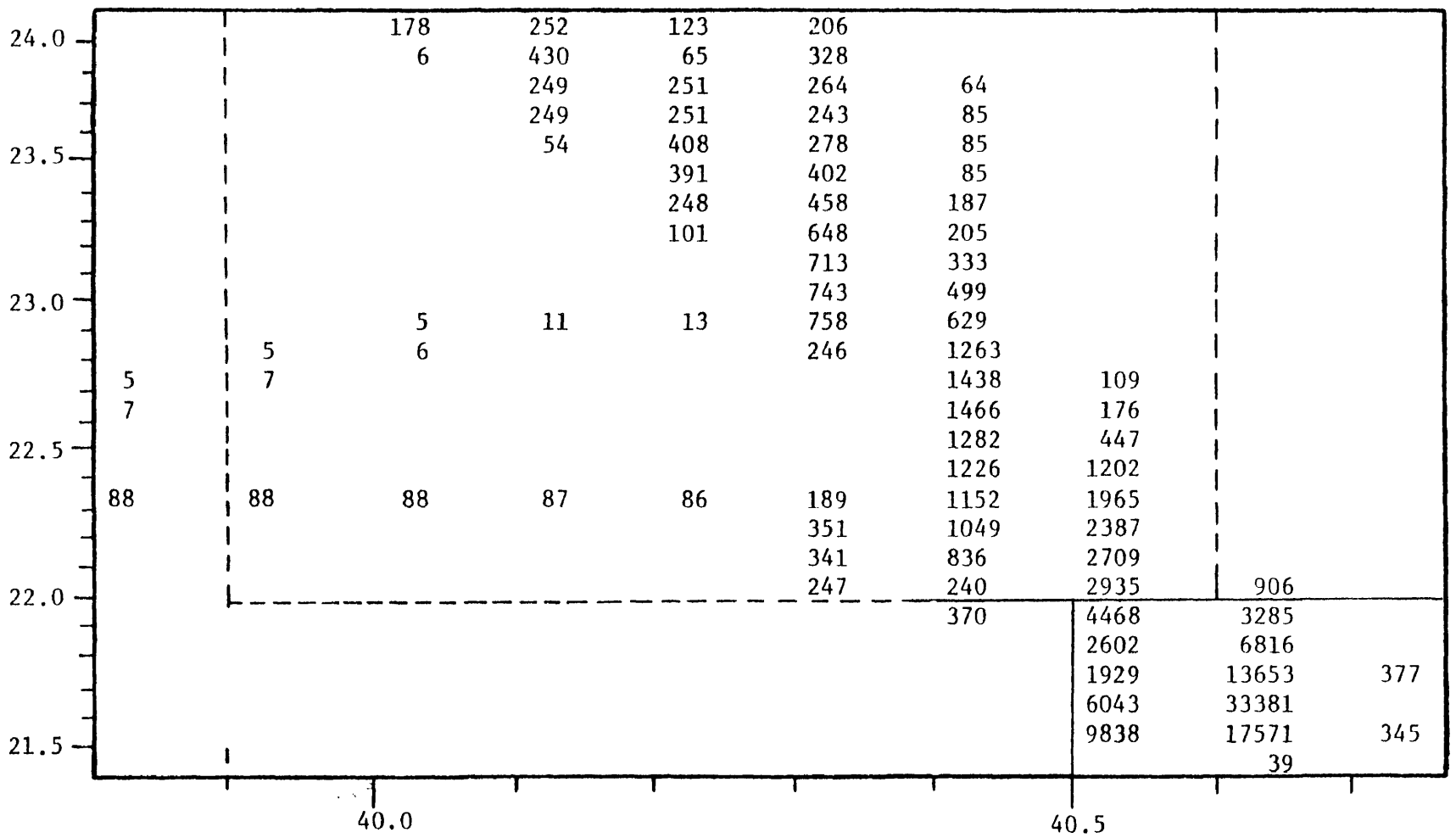

Figure 6. Detailed volumetric temperature/salinity census of Red Sea water for summer. Values indicate volumes in km^3. This figure is a detailed expansion of the lower right section of figure 6.

R.S.B. water 57% = 100347 km^3

R.S.I. water 19% = 33851 km^3

	39.9	40.0					40.5			
24.0	293	139		235	36					
	292	107	32	127	151					
	127	2097	138	163	177					
		1150	77	491	359					
	22	401	159	436	1352					
23.5	25	134	444	144	1360	35				
		30	457	113	225	945				
			290	447	147	775				
			230	171	816	2905				
				268	120	2720				
23.0				267	119	1649	423			
				266	82	508	1351			
				79	186	550	1516			
					264	250	1889			
	18				264	58	2376			
22.5	3	5			88	175	2191			
		1	4			400	2150	12		
			1	4		490	1850	511		
				2	3	487	752	2247		39
22.0					2	486	394	3318		74
						48	594	8067	294	286
							1511	6826	6616	515	122
							1211	16567	8360	952	
21.5								30909	6052		
								2935	518		

Figure 7. Detailed volumetric temperature salinity census of Red Sea water for winter. Values indicate volumes in km^3. This figure is a detailed expansion of lower right section of figure 14.

R.S.B.W [55%] = 92335 km^3

R.S.I.W [28%] = 48273 km^3

Water accounts for 28.2% of the total volume during winter, while the Upper Water Mass accounts for 8.1% of the total volume, seasonal relationships of these water masses are shown in Table 1. The temperature and salinity limits of this water mass have been lowered to 24.0-27.0°C and 38.0-40.1‰ to accommodate the effects of reduced air temperatures in winter and freshening by incoming less-saline water from the Gulf of Aden.

Table 1. Volume as a Percent of the Three Main Red Sea Water Masses Identified Seasonally.

Season	Red Sea Bottom Water	Red Sea Intermediate Water	Red Sea Upper Water	Others and Mixtures
Summer	57.4%	18.5%	5.1%	19%
Winter	53.3%	28.2%	8.1%	10.4%

Water Type Analysis

Summer Season

Parent Type A

Water type A occupies an intermediate layer, between 50 and 100 m, with highest concentration at 75 m in the vicinity of the sill. This water represents the influence of Gulf of Aden on the Red Sea during summer. Its concentration decreases after the second segment. One can easily see in Figure 8 that this water is originally found at intermediate depths in the Gulf of Aden.

Parent Type B

During the summer water type B fills the greater part of the Red Sea basin. Very little of this water is found at the surface in all segments, including the Gulf of Suez. Figure 9 shows isopleths of equal concentration of water type B elevated at the northern end of

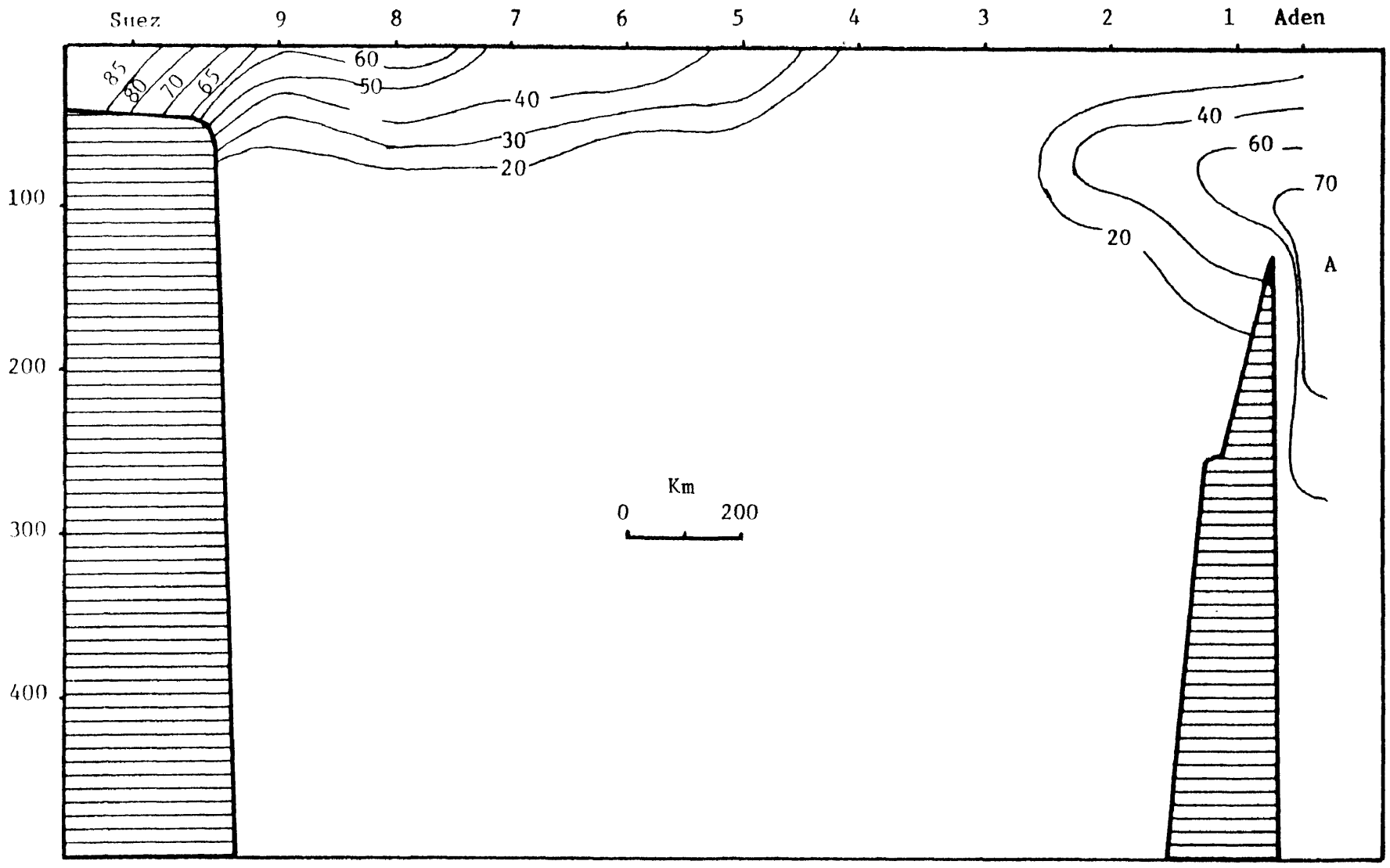

Figure 8 . Parent types A and C distributions for summer.

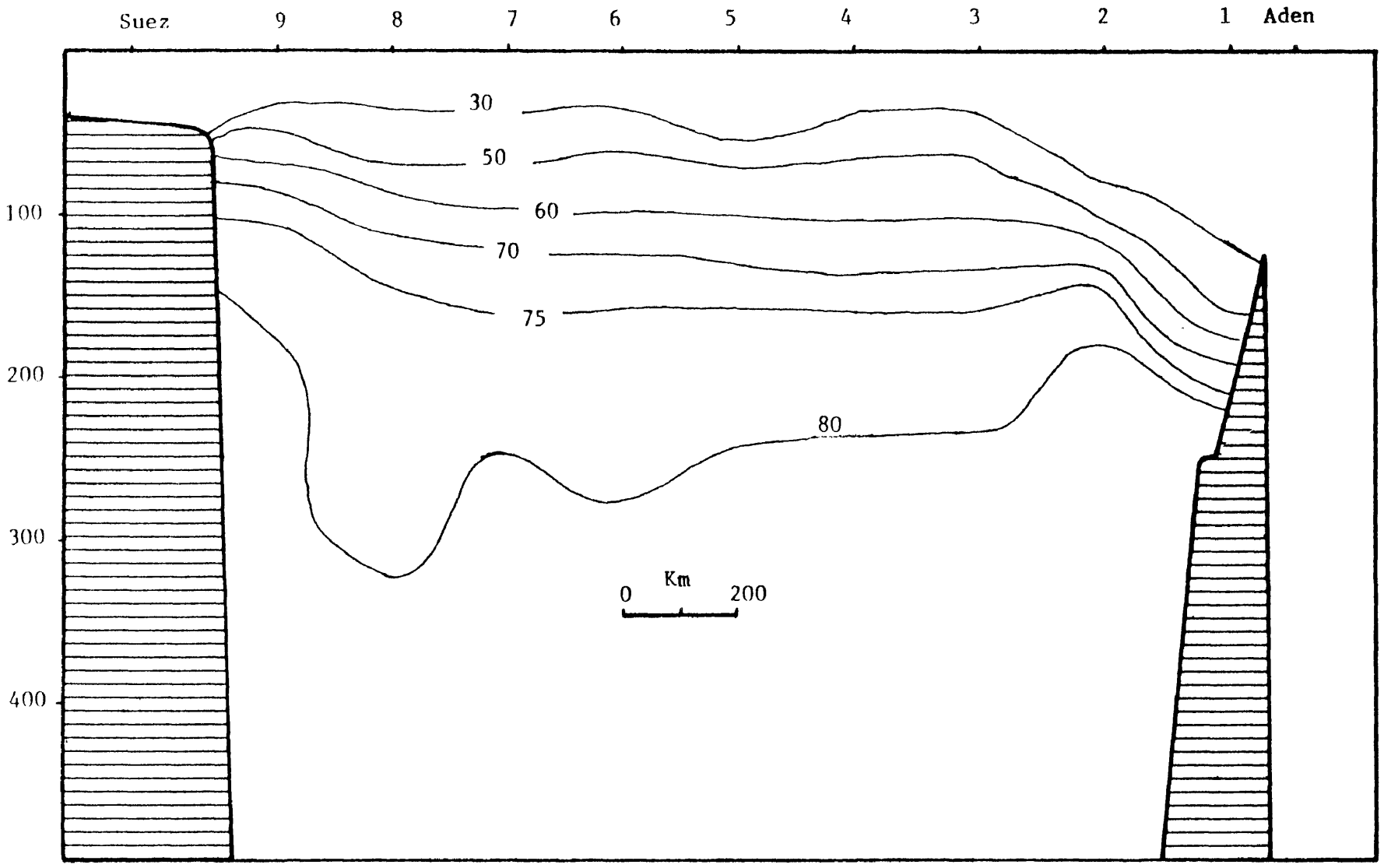

Figure 9 . Parent type B distributions for summer.

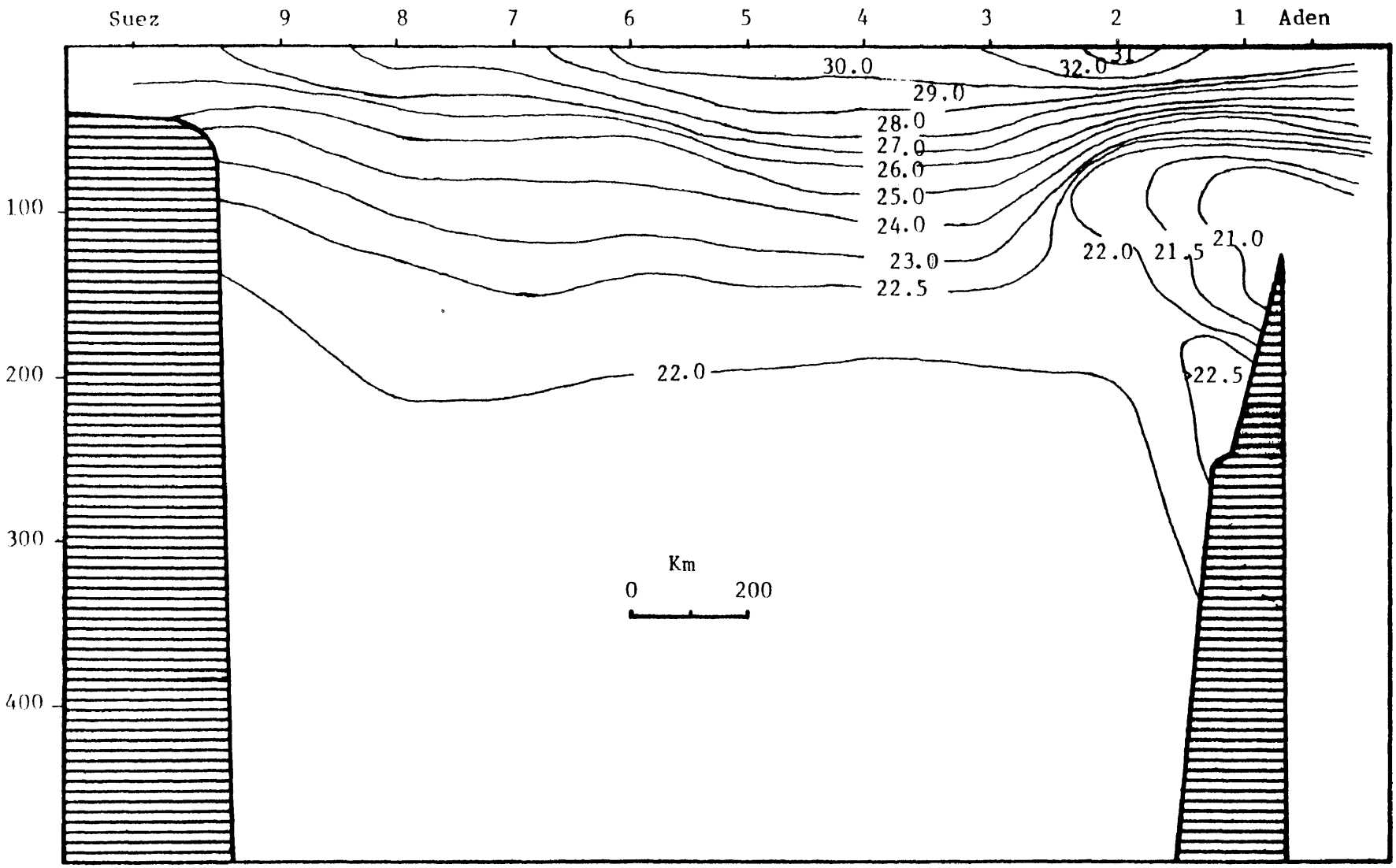

Figure 10 . Temperature distributions along the central axis of the Red Sea for summer.

the basin (segment 9). These upward slopes are in agreement with the summer temperature (Figure 10) and show a response to wind driven surface transport towards the south in summer. However, this process is not sufficiently strong to cause upwelling from great depths as can be seen in Figures 9, 10 and 11. Depths of isopleths are shallow during this season (the 80% isopleth has a mean depth of 250 m) indicating an increased volume of this water, which is in agreement with the summer volumetric census. Another upward slope of water type B isopleths towards the south is found in segment 2 indicating this water piles up in front of the sill. This is because the incoming water from the Gulf of Aden at depth impedes the exiting of water type B over the sill.

Parent Type C

Parent water type C, with T = 26.0 and S = 41.6$^{o}/oo$, represents Gulf of Suez influence upon the Red Sea during summer. It originates in the Gulf of Suez during summer and occupies the upper 50 m of the water column in the northern region (Figure 8). Leaving Gulf of Suez, it remains concentrated at the surface in segments 7, 8 and 9. It is driven by wind stress southward as far as segment 4 and, despite its high salinity, remains positively buoyant because of its elevated temperature.

Parent Type D

With a high heat exchange between the surface layer and the atmosphere, surface water attains the highest temperature in the region to form water type D. The greatest concentration of this parent water type is centered around segment 2 (Figure 12) and it occupies the upper

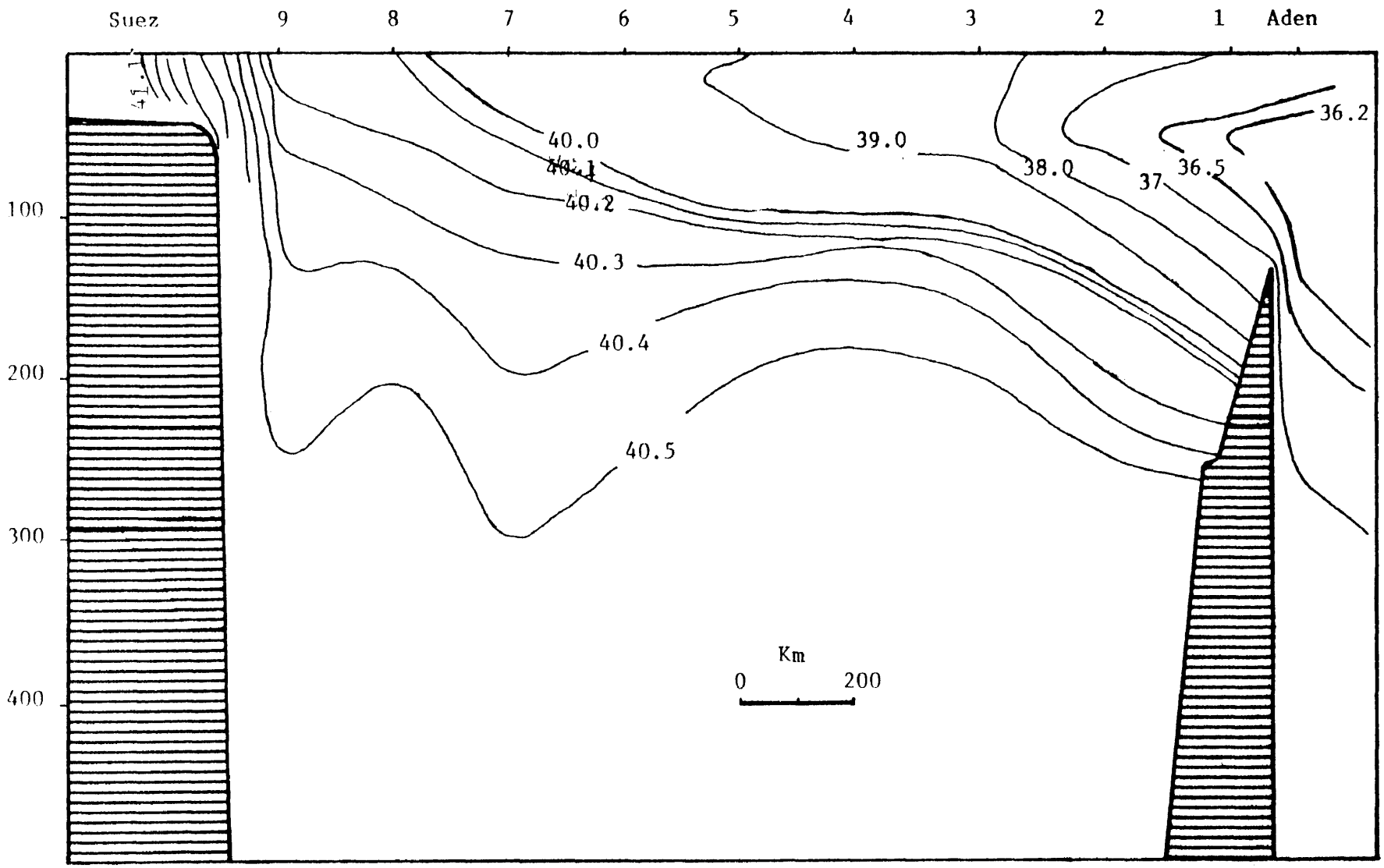

Figure 11 . Salinity distributions along the central axis of the Red Sea for summer.

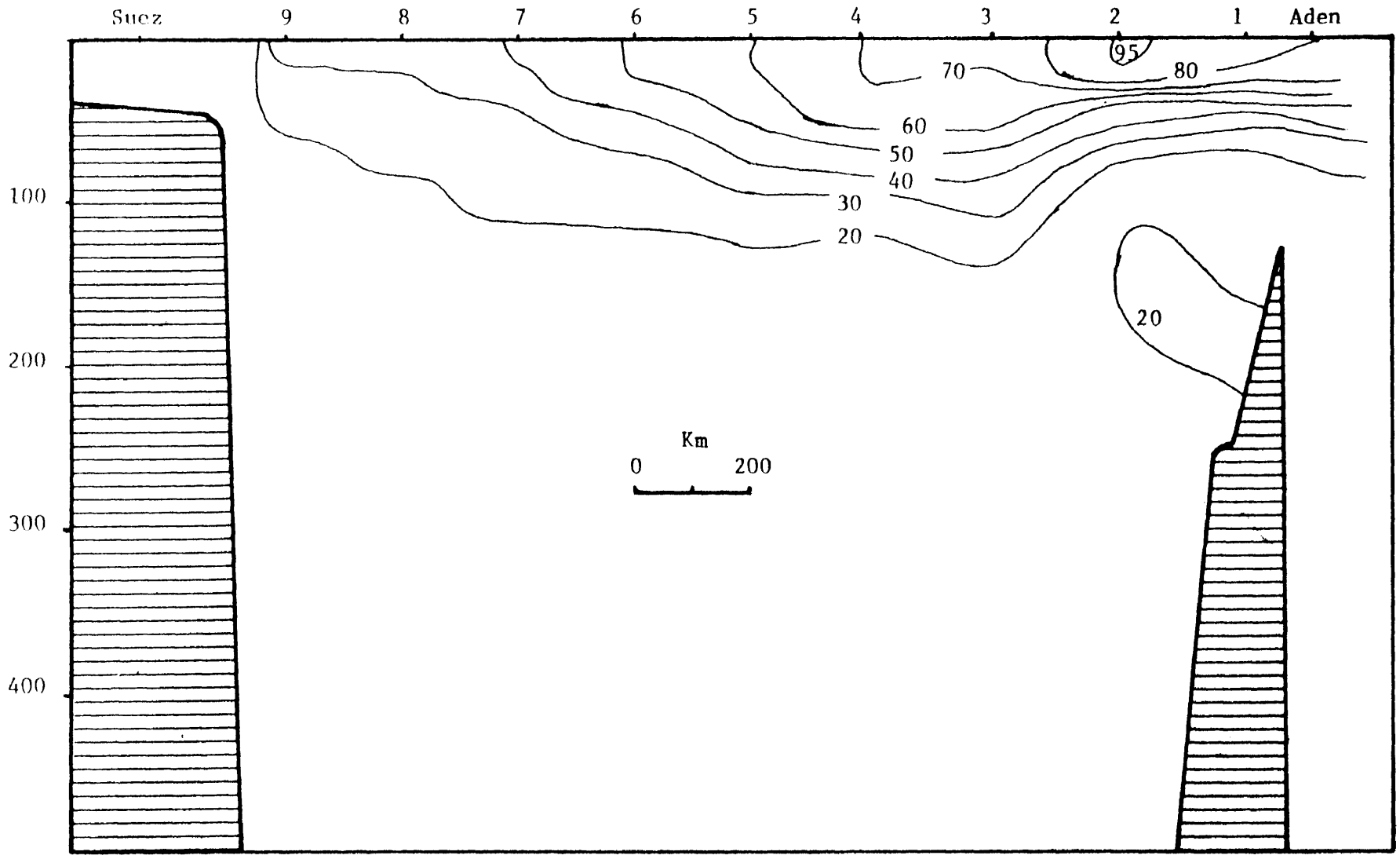

Figure 12 . Parent type D distributions for summer.

50 m of the water column in the Gulf of Aden and segments 1 through 6. This water is driven by the wind out of the Red Sea into the Gulf of Aden. Isopleths of concentration of this water have an upward slope around the sill indicating that its confined to a thin layer as it leaves the Red Sea. This upward slope around the sill can be caused also by an incoming subsurface flow from the Gulf of Aden during this season.

Winter Season

Average winter distributions of temperature and salinity in the Red Sea are shown in Figures 13 and 14. These distributions, cast as water type analyses, yield the following:

Water Type B

During winter, parent water type B has the highest concentration, 90%, at the Gulf of Suez, its source region, Figure 15. Very little of it is found in the upper 50 m of segments 1 through 4 and the Gulf of Aden. In the vicinity of the sill, isopleths of concentration of this water slope sharply downward towards the Gulf of Aden. Although very little of this water type is found at the surface in the Gulf of Aden, it reaches higher concentration with increasing depth. A sharp upward slope is found around segment 6. This sharp slope decreases with increasing depth suggesting upward motion at intermediate depths. In contrast to summer, isopleths of a given concentration of Red Sea Bottom Water are deeper (compare Figures 9 and 13) indicating decreased volumes of this water, which agrees with the winter volumetric census (Figure 5) and Table 1.

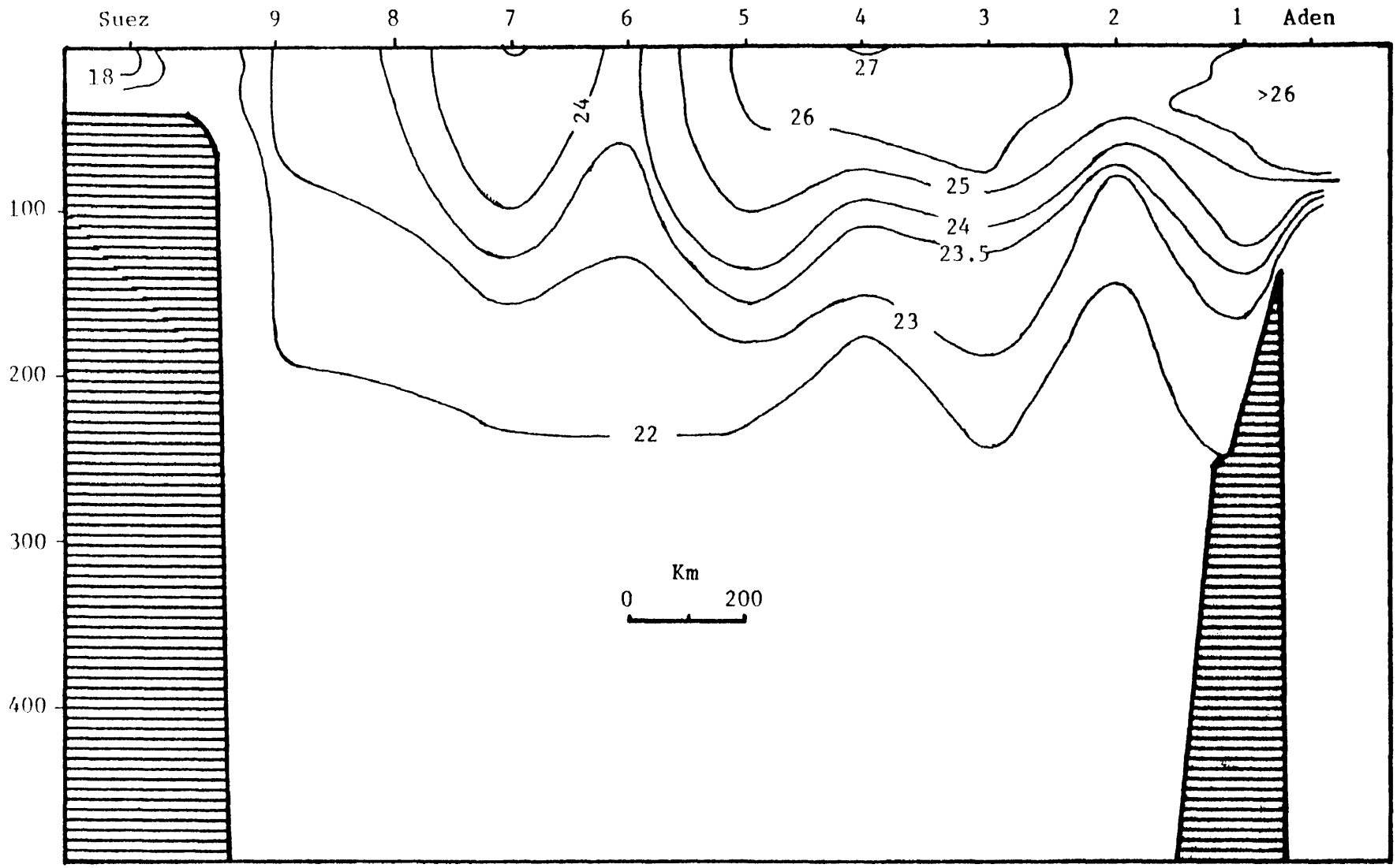

Figure 13. Temperature distributions along the central axis of the Red Sea for winter.

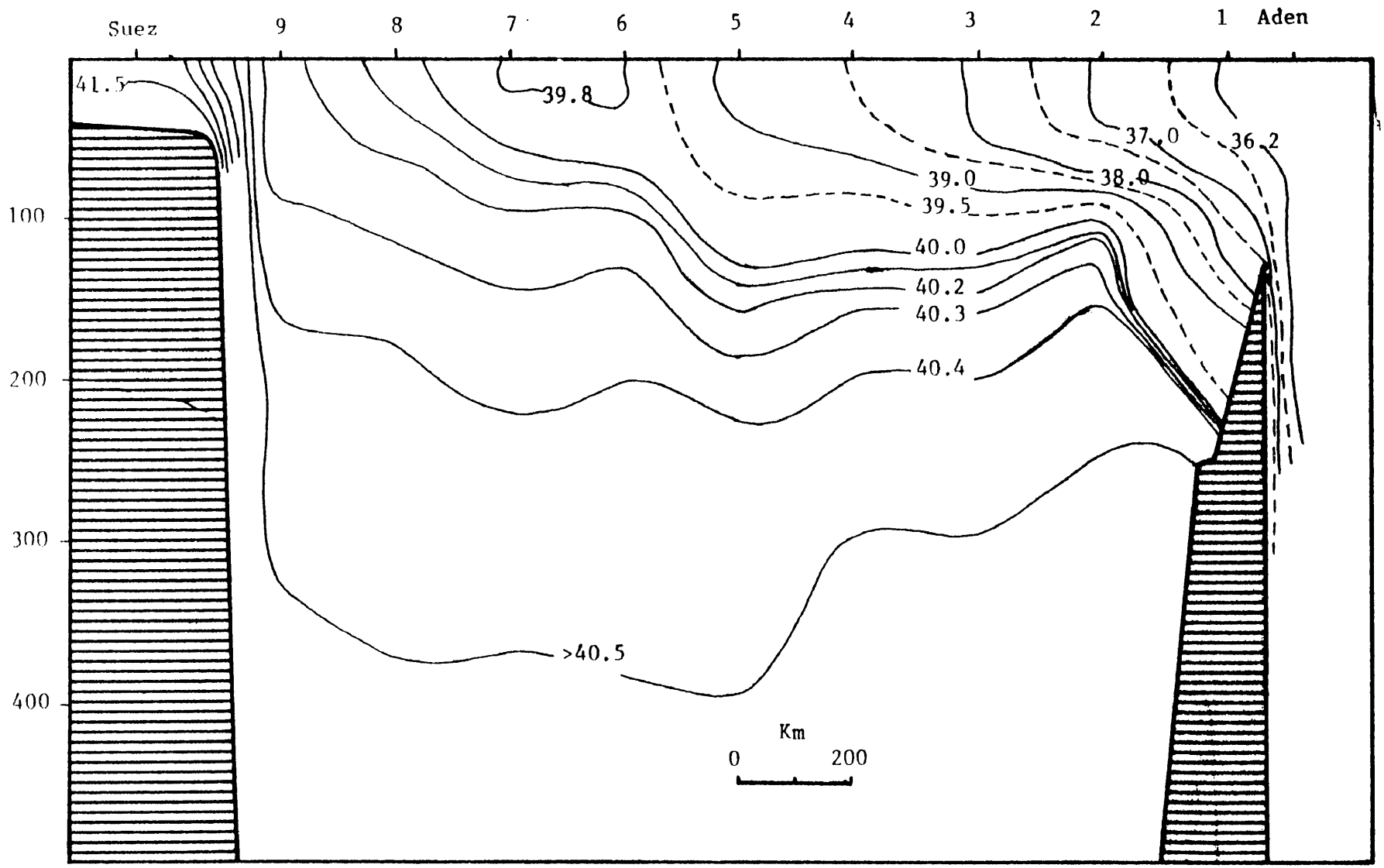

Figure 14 . Salinity distributions along the central axis of the Red Sea for winter.

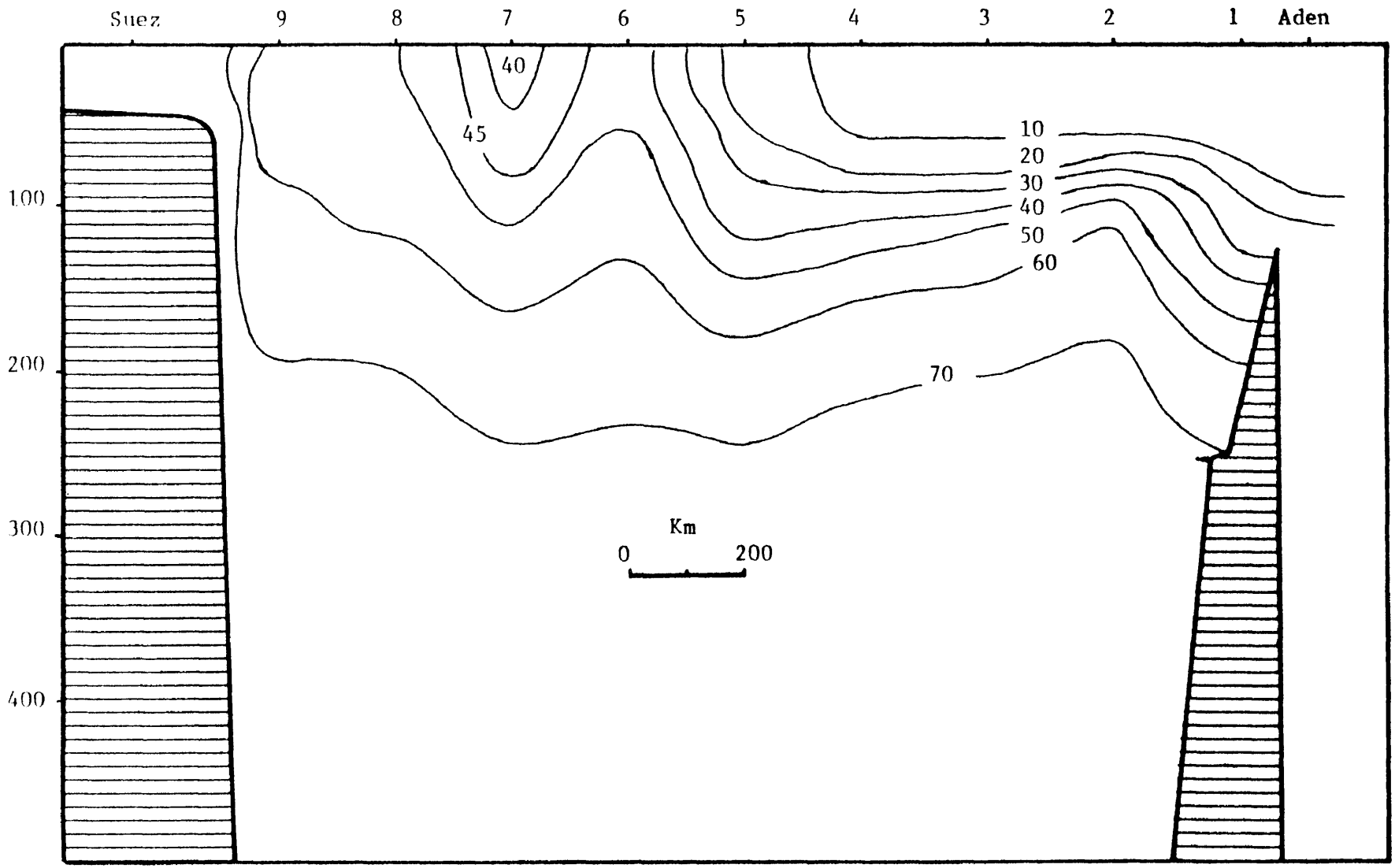

Figure 15 . Parent type B distributions for winter.

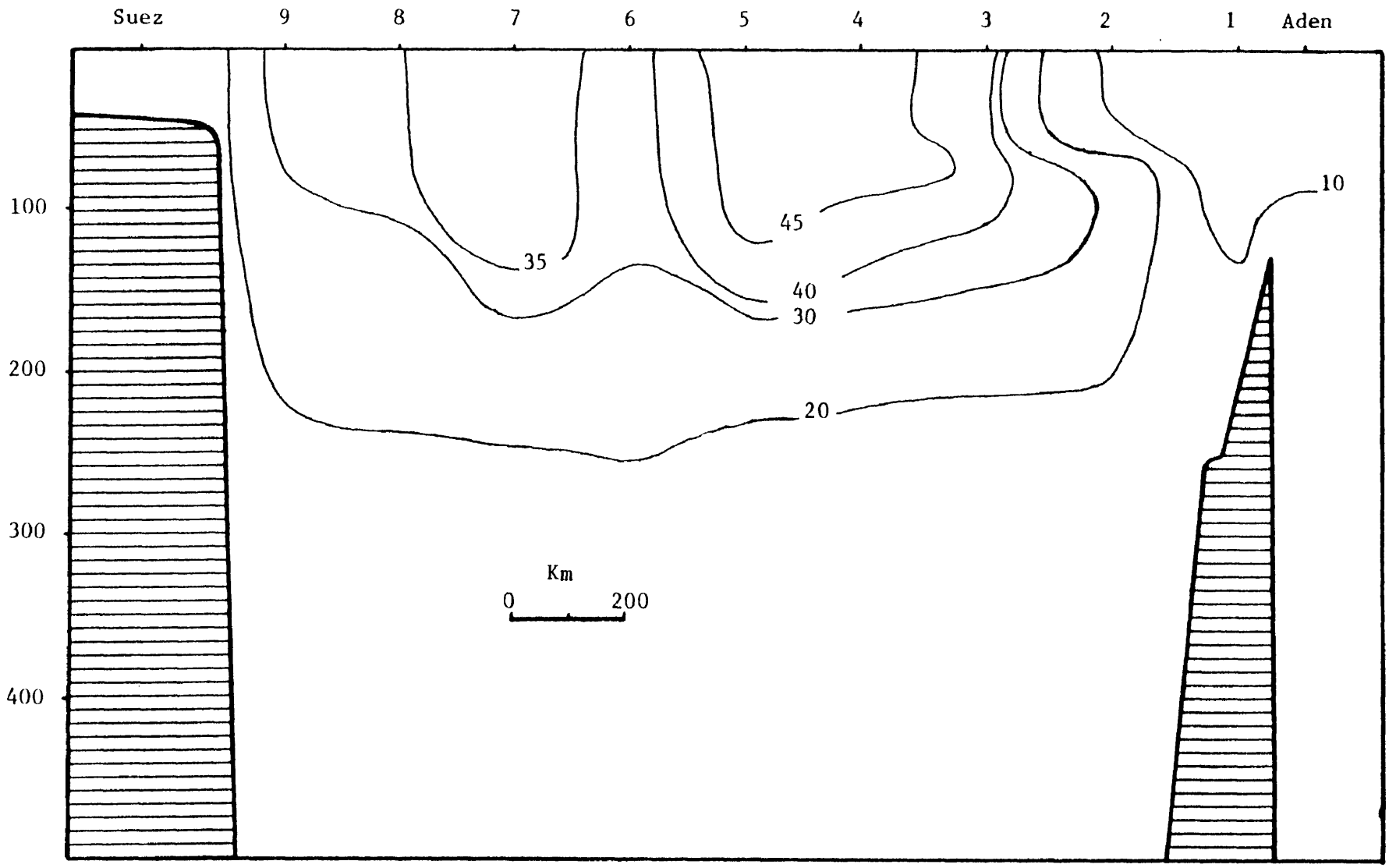

Figure 16 . Parent type E distributions for winter.

Water Type E

Water type E is a mixture of summer water types C and D in a 73:27 ratio (C:D). Figure 16 shows that during winter, this water is concentrated as two envelopes. The first occupies the upper 100 m in segment 5 while the second is in segment 7. Isopleths of water type E in segments 2, 3 and 4 are forced northward at the surface whereas at a depth of 100 m they extend southward indicating movement towards the sill as a subsurface flow. These envelopes are originally formed as mixtures of summer parent water types and eventually move southward towards the sill.

Parent Water F

Parent water type F is also a mixture of two summer water types, D and A, in a ratio of 53:47. It occupies the upper 100 m of the water column with highest concentrations (>95%) found in the upper 50 m in the vicinity of the sill as shown in Figure 17. This water decreases in concentration as it extends northward into the Red Sea and with depth. Isopleths of concentration of water type F incline northward at the surface whereas they tend to be deeper towards the south. This water is driven by wind stress into the Red Sea from the Gulf of Aden, where the original parent water types D and A are formed during summer season. Very little of this water is found in the Gulf of Suez.

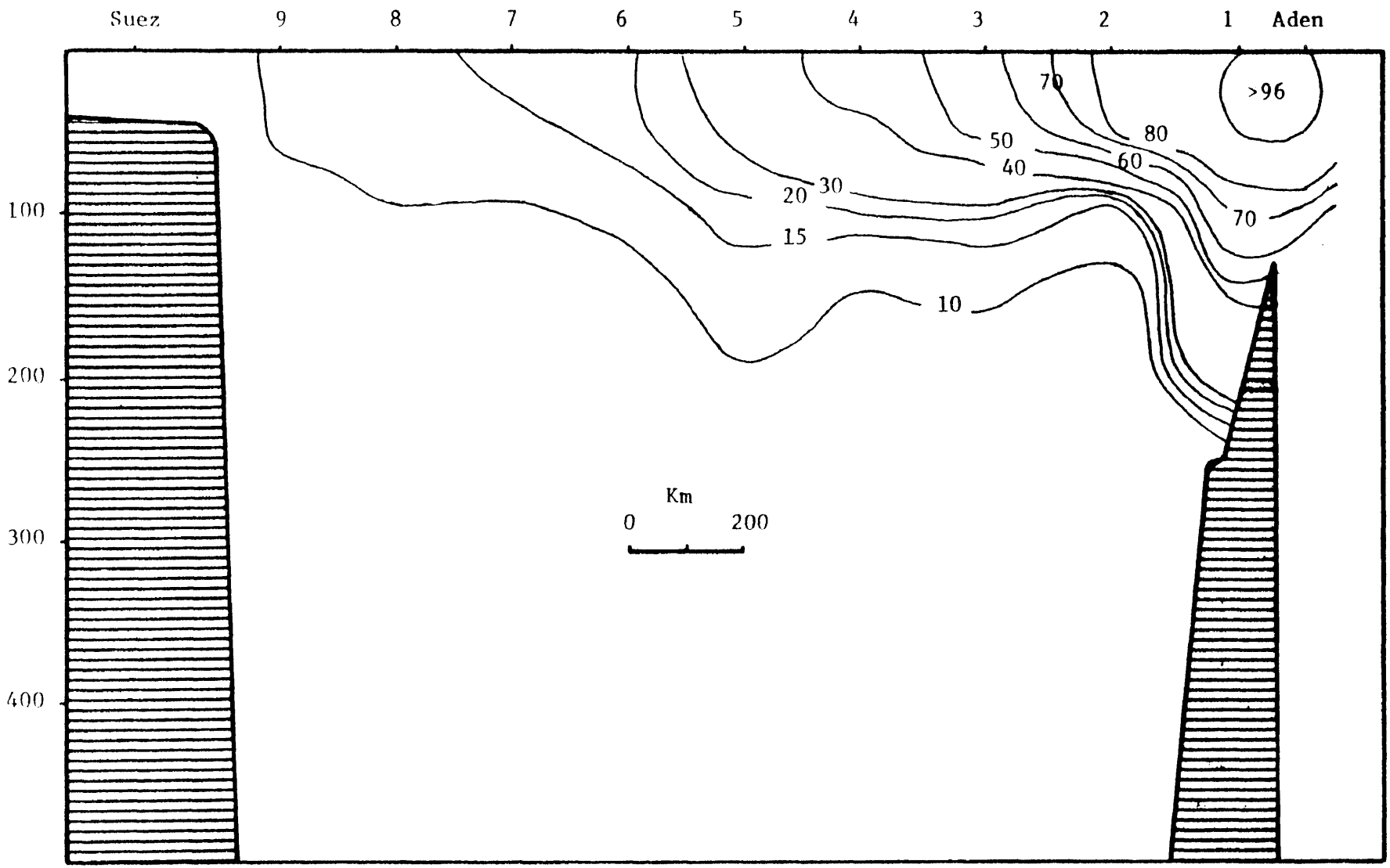

Figure 17 . Parent type F distributions for winter.

IV. DISCUSSION

The increased volume of the Red Sea Upper Water mass from summer to winter is due to a larger inflow from the Gulf of Aden during winter resulting from wind stress acting on the surface layer and the northerly directed pressure gradient resulting from water loss in the northern part. Although independent, these forcing functions reinforce each other.

Red Sea Intermediate Water increases in volume during the same period (summer to winter). This increase in volume is a consequence of stronger mixing between the surface and deeper water which is the result of accelerated evaporation during winter. Red Sea Bottom Water decreases in volume during winter. Isotherms shown in Figure 13 slope downward towards the sill in segment 2 and reverse direction as the sill is approached. It can be seen from this figure that the upper 125 m in the vicinity of the sill contains two layers: A surface incoming flow from the Gulf of Aden and a subsurface outflow from the Red Sea. Thus, during winter a mixture of the Red Sea Bottom Water and Red Sea Intermediate Water moves over the sill and out of the Red Sea. This in- and out-flowing water is also evident from the winter isohaline configurations (Figure 14). In the surface layers, isohalines are inclined upward towards the north indicating surface inflow from the Gulf of Aden while at depth, the isohaline tilt is reversed, an indication of the outflow of deeper water in segment 1. Thus, Red Sea Bottom Water that forms during winter in the Gulf of Suez mixes with

surface water and is exported via the bottom to the Gulf of Aden as Red Sea Intermediate Water. This winter circulation pattern poses a question: If Red Sea Bottom Water is formed during winter, why is its volume greatest during summer?

During summer, winds are from the north northwest over the entire Red Sea basin and drive surface water into the Gulf of Aden as indicated by isotherms shown in Figure 10. This outflowing water is replaced by water from intermediate depths at the northern end of the basin. Isotherms at this end slope upward indicating this process. At the southern end, at a depth of 150 m between segment 2 and 3, isotherms are divided into two groups. The upper group near the surface is elevated towards the south because of incoming water from the Gulf of Aden at intermediate depths which also depress isotherms in the Red Sea below 150 m at the southern end. The 22° isotherm, marking the upper limit of the Red Sea Bottom Water, slopes sharply downward towards the south between segments 1 and 2 indicating that during summer this water never reaches the sill and is trapped within the basin. This explains the larger volume of Red Sea Bottom Water during the summer. Thus the summer circulation pattern in the vicinity of the sill is composed of two layers: outflowing surface water from the Red Sea into the Gulf of Aden and inflowing subsurface water from the Gulf of Aden. This circulation is also indicated by the isohalines configurations shown in Figure 11.

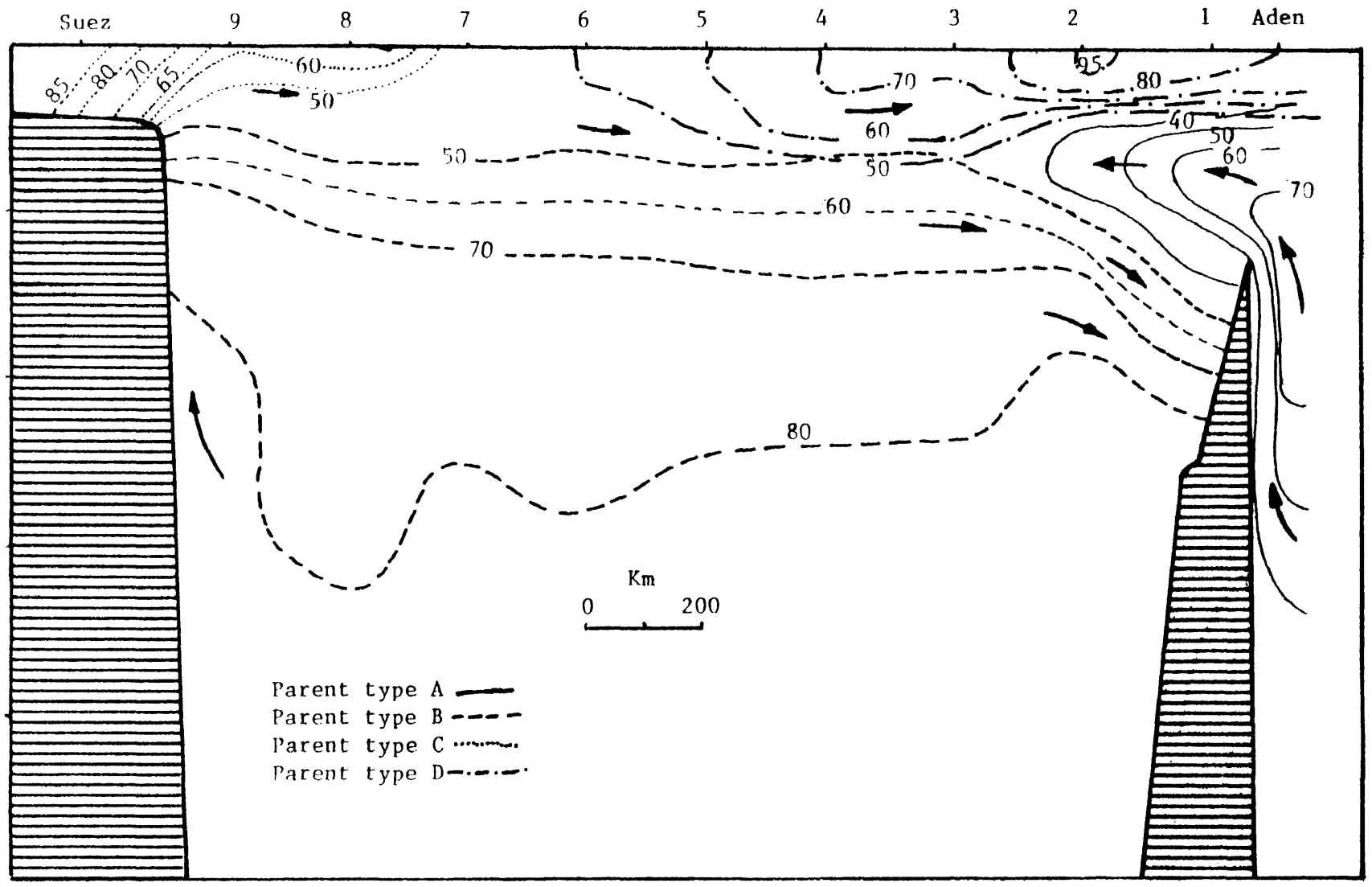

Figure 18. Distributions of parent types A, B, C and D in the Red Sea during summer. Arrows indicate implied water motion.

Water Type Analysis

Average Summer Conditions

The four parent water types present in the Red Sea during summer are types A, B, C and D. As a subsurface layer, water type A is found in the Gulf of Aden and segments 1 and 2, Figure 18. The surface layer in the Gulf of Aden and in segments 1 through 6 is dominated by water type D. The surface layer for the remainder of the Red Sea (segments 7 through 9) and the Gulf of Suez, is occupied by parent water type C. Below 200 m the whole region is occupied by parent water type B. As shown in Figure 18, the surface layer in the Red Sea is actually a combination of parent types D and C. The region between segments 6 and 7 is occupied by a mixture of D and C. The elevated temperature of this water during summer is explained by the high temperatures of the forming parental water types D and C. Higher temperatures of parent type D are due to higher heat exchange between the atmosphere and the surface layer in the southern region while the elevated temperatures of water type C resulted from more intensive heating of the shallow body of water of the Gulf of Suez. When the Surface Layer mixes with the subsurface water (type B) Red Sea Intermediate Water is formed in a 50 m thick layer. From Figure 18 one can see that neither water type B nor Red Sea Intermediate Water can flow over the sill. In the vicinity of the sill the incoming water, type A, at depth is actually blocking the way out for water type B or Red Sea Intermediate Water. Isopleths of water type B are forced downward towards the sill by water type A entering from the Gulf of Aden. This subsurface inflow reaches as far north as segment 3. Its volume is

relatively small (approximately half of one percent of the total Red Sea volume) and it forms the cold tongue of water in this region observed by Everett and Browning (1971). Winds over the length of the Red Sea drive the surface layer into the Gulf of Aden. In response to this surface water removal, compensatory upward motion is evident in the northern portion of the Red Sea where water which is found at depths of 300 m in the main portion of the Red Sea is elevated to depths of 100 m (see also Figures 9 and 10).

Average Winter Conditions

The three parent water types present in the Red Sea during winter are B, E and F. The latter two are each mixtures of pairs of summer water types. E is a mixture of types D and C while F is a mixture of types D and A. Figure 19 shows that in the Gulf of Aden and segments 1 through 4, the surface layer is dominated by parent water type F. As this water spreads northward it becomes shallower. Between segments 4 and 5 the upper 100 m is occupied by water type E as are the upper 100 m between segments 7 and 8. Segment 6 contains a mixture of different water types in which the dominant water type is not surface water but subsurface water type B.

Between segments 4 and 8, winter surface winds and associated Ekman drift combine with the effects of evaporative loss, particularly from the Gulf of Suez, to produce a cyclonic circulation of surface water. This cyclonic eddy is centered around segment 6. Diverging surface water within this eddy is replaced by upward movement of subsurface layers. This upwelled water is mainly water type B and occupies the region between segments 8 and 9. Thus, during winter the upper

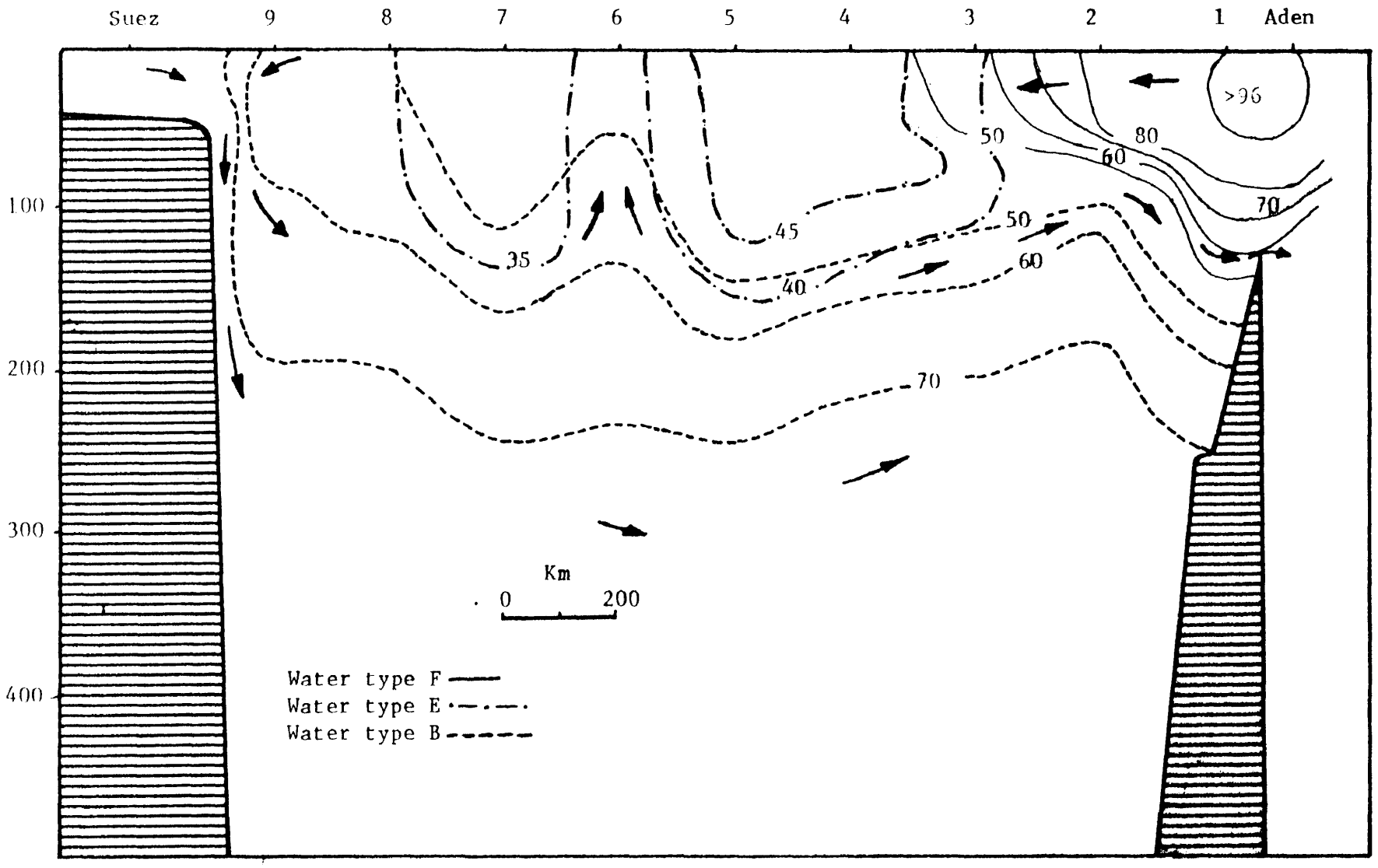

Figure 19. Distributions of parent types E, F and B in the Red Sea during winter. Arrows indicate implied water motion.

water mass is a mixture of types A, B, C and D since E is a mixture of C and D and F is a mixture of A and D. Water type E shifts from its summer position between segment 6 and 7 to a winter location indicating a southward movement from summer to winter. Water type B shows a decrease in volume in the Red Sea during this season despite the fact that conditions favor its formation (see Figures 17 and 18).

Circulation

Summer

During summer, in the northern region, parent type C, from the Gulf of Suez, is driven southward. This water with $t = 26.0^{\circ}C$, $S = 41.6$ and $\sigma_{\theta} = 27.0$ is lighter than the subsurface water and, thus, stays at the surface. With southerly directed wind over the entire length of the Red Sea the whole Red Sea surface is divergent from the northern end. This divergence from the north causes water to be upwelled from depth as indicated in Figures 9 and 10. In the northern region, water from the Gulf of Suez mixes with water type D accounting for water type E. This water, E, occupies the region between segments 6 and 8 and is driven by wind towards the south. In the southern region, water at the surface is driven by wind out of the Red Sea into the Gulf of Aden where it mixes with Gulf of Aden surface water. At this time in the Gulf of Aden, deep Arabian sea water is upwelled and present along the southern coast of Arabia and Somali. This upwelled water, parent type A, is the major component that goes into the Red Sea at the bottom layers across the sill. Thus the summer circulation pattern is as follows: outflowing surface water, from the northern end, and over the sill into the Gulf of Aden and inflowing subsurface

waters from the Gulf of Aden and over the sill into the Red Sea as far north as segment 3. This circulation is indicated by the isohalines and isotherms configurations in Figures 10 and 11.

Winter

During winter, surface winds, in the northern portion of the Red Sea are from north northwest while in the southern portion they blow from the opposite direction forming a convergent region between 19 and 21°N. When north northwest cold dry wind blows over the northern region of the Red Sea, the surface layer attains higher density ($\sigma_\theta \approx 28.0$) as a result of cooling and evaporative losses. The difference in σ_θ between the surface and the underlaying water is less than a 0.1 of a unit and may cause an overturn. However, this is of minor importance and cannot account for the deep water formation. The surface layer on the eastern side of the northern portion of the Red Sea is entrained by the cyclonic circulation and meets with the water coming out from the Gulf of Aqaba. When these two currents meet at segment 9 a convergence occurs which can be seen in Figures 13, 14, 15 and 18). This convergence does not extend below 200 m as illustrated in Figure 13 indicating that the cyclonic circulation cannot be responsible for the Red Sea Bottom Water formation. The final possible source of bottom water is the Gulf of Suez. Water here attains a temperature of 18.0^{o}C and salinity of 41.5 ($\sigma_\theta \approx 30.0$) in winter. When this water enters the Red Sea (near 28°N) it mixes with the surface layer ($\sigma_\theta \approx 28.0$). The mixture of those two water types has a density of water at a depth of 900 m in the Red Sea. Thus

the Red Sea Bottom Water is not caused by evaporative process acting on Red Sea Surface Water at the northern region. Rather, water from the Gulf of Suez, mixes with the Red Sea Surface Water to form the bottom water.

V. CONCLUSIONS AND RECOMMENDATIONS FOR FUTURE WORK

This study was undertaken to answer the following questions through analysis of available data:

> What are the predominant and the secondary water masses present during the warm and cold seasons in the Red Sea?
>
> What is the extent of the exchange between the Red Sea and the Gulf of Aden through the Straits of Bab el Mandeb?
>
> Are the water masses formed in the Red Sea or are they the result of advection?

The first question was answered by analyzing summer and winter volumetric T/S census for the Red Sea. Water in the Red Sea basin is dominated by a single mode, Red Sea Bottom Water, with $T = 21.5\text{-}22.0^{\circ}C$, $S = 40.5\text{-}40.7^{o}/oo$. This water mass accounts for 53.3 and 57.4% of the total volume in the Red Sea during winter and summer seasons respectively and occupies the region below the 200 m isobath inside the Red Sea.

The second largest mode represents Red Sea Intermediate Water with $T = 22\text{-}24^{\circ}C$, $S = 39.9\text{-}40.5^{o}/oo$ which accounts for 18.5% and 28.2% of the total volume during summer and winter respectively.

The Red Sea Upper Water, a newly defined water mass, occupies the upper 100 m and accounts for 5 and 8% of the total volume during warm and cold season respectively. It is a mixture of three parent water types, Red Sea surface water, Gulf of Suez summer water and Gulf of Aden intermediate water in summer.

The remaining questions are answered by employing a water type analysis.

Two parent water types originate in the Gulf of Suez and are called Suez winter and summer parent water types. A single parent water, Gulf of Aden Intermediate Water, originates in the Gulf of Aden. A new parent water type originates in the Red Sea during summer: Red Sea Surface Water.

All these water types account for the formation of water masses in the Red Sea.

Red Sea Bottom Water originally from Suez winter, mixes with Red Sea Surface Water and accounts for the second largest mode, Red Sea Intermediate Water. Red Sea Surface Water by mixing with the Gulf of Aden Intermediate Water accounts for the incoming water from the Gulf of Aden during winter at the surface. The upper water mass in both seasons is a mixture of three parent types: Red Sea Surface water, Aden Intermediate Water and Suez Summer Water.

The extent of exchange through the Strait of Bab el Mandeb varies seasonally. During summer, as a bottom inflow at the sill, Gulf of Aden Intermediate Water reaches as far as 17°N as a shallow layer and has a very small volume compared to the total Red Sea volume. During winter the volume of the incoming water, a mixture of Red Sea Surface Water and Gulf of Aden Surface Water, is larger and extends as far as 17°N with an average thickness of 70 m.

The Gulf of Suez is very small by volume compared to the Red Sea but plays a dominant role on water mass formation. During winter, in the Gulf of Suez, with a cool dry wind, evaporation is at maximum

resulting in the formation of dense water $\sigma_\theta \approx 30$. A deep convection current is accentuated when this heavy water from the Suez mixes with surface Red Sea water ($\sigma_\theta \approx 28.0$) north of 27°N. The resulting mixture has a density equal to the density of water found between 900 to 1000 m. Thus, Red Sea Bottom Water originates, in part, as Gulf of Suez winter water, parent type B. The Gulf of Suez accounts for another water mass that flows southward, not less than 24°N, before it is absorbed through mixing with adjacent water masses.

Thus Red Sea Bottom Water, Red Sea Intermediate Water and Red Sea Surface Water are all formed in the Red Sea and dominate the whole region while the upper water mass is a mixture of locally formed, Red Sea Surface Water, with non resident Suez and Aden water. The Gulf of Aqaba does not play a significant role in the Red Sea Bottom Water mass formation. Surface water from the southern region brought to the northern part by the cyclonic circulation along the eastern shore mixes with the incoming water from the Gulf of Aqaba and forms more of the Red Sea Intermediate Water.

Thompson (1939a) made the first attempt to determine the method of Red Sea Bottom Water formation. He stated that the Red Sea Bottom Water must be formed north of 26°N by evaporative processes. Although he was the first investigator to attempt to find the origin of Red Sea Bottom Water, he did not give a reasonable explanation of how this water is formed. His data was collected as far north as 26° in winter. It is the opinion of this author that he assumed this water must be formed north of 26°N. A second attempt to identify the source of the Red Sea Bottom Water was made by Neumann and McGill (1961). They

discussed the circulation of the Red Sea in early summer and reported that "...water of maximum density should form at the surface in the north during the winter months when evaporation and cooling are both at a maximum. This would account for the deep water of 21.7°C and 40.6‰ in the Red Sea basin below sill depth". Data sets used in their analysis were collected in mid-June. With a well-defined cold season from December to March, June should fall in early summer. They argued that winter circulation was still persistent in June. Having no hydrographic stations from the Gulf of Suez, they reached the same conclusions as Thompson (1939a): Red Sea Bottom Water originates in the northern part of the Red Sea.

It is quite clear now from this investigation that the conclusions of Neumann and McGill (1961) and Thompson (1939a) are only partly correct. It is the water from the Gulf of Suez (T = 18.0°C, S = 41.5‰, $\sigma_\theta \approx 30$), which plays an important role in forming Red Sea Bottom Water. Water originating in the Gulf of Suez during winter mixes with surface water at 28°N. The density of this mixture is higher than the surface layer at 28°N, and it sinks to a stable depth of 900-1000 m. Thus, it is the dense winter water from the Gulf of Suez that mixes with Red Sea Surface Water to form the deep water. This mixture contains 10% Suez Winter Water (type B) and 90% Red Sea Surface Water from 28°N (T = 22.0°C, S = 40.4‰) which produce Red Sea Bottom Water which, on the average, represents 55% of the water in the Red Sea (93,950 km^3). To produce this mixture, the Gulf of Suez must contribute 9,393 km^3 of winter water. According to Patzert (1972), winter outflow from the Gulf of Suez has an average strength of 5 cm s^{-1}

which would result in a volume discharge of 650 km^3 per winter season. At this rate, it would take 15 years for the formation of the average measured volume of Red Sea Bottom Water. This is comparable to Seidler's (1969) estimate of 20 years. Water from the Gulf of Aqaba has σ_θ = 28.5. This water mixes with water from the southern region, driven by the cyclonic circulation northward along the Arabian side of the Red Sea to form Red Sea Intermediate Water. This mixture finds its density between 200-250 m.

Thompson (1939a) and Patzert (1972) concluded that during summer, water over the sill is divided into three layers. At the surface a thin layer is driven out of the Red Sea and into the Gulf of Aden; an incoming flow from the Gulf of Aden occurs between 40 and 100 m and another outflow, deeper than 100 m, transports water from the Red Sea into the Gulf of Aden. The outflowing at the bottom, in the vicinity of the sill, was assumed to be Red Sea Bottom Water. If their analysis are correct one would expect to find a reduction in the volume of Red Sea Bottom Water during the summer. The volumetric T/S census shows the opposite. Isotherms during this season (Figure 3) show no evidence of a three layer circulation system near the sill. The present analysis shows a two layer circulation system persists in both seasons with each layer reversing direction from summer to winter.

Suggestion for Future Work

The predominant thrust of recent oceanographic research on the Red Sea has been towards the study of hot brines (for a complete reference see Monin and Plakhin, 1982). Water exchanges through the Suez Canal have largely been neglected when compared to the attention

given to the exchange with the Gulf of Aden through Bab el Mandeb. This exchange, through the Suez Canal, was increased recently by the 1979 deepening and widening of the Suez Canal. The resulting new exchange rate should have some physical, biological and chemical effects on the environments of both the Mediterranean and the Red Seas. To study these new conditions and their environmental impacts, a systematic program of data collection and analysis is needed during the present decade. To determine the total water budget of the Red Sea more prolonged direct current measurements are needed. The current observations should be made in the vicinity of the sill near Hanish Island, in the straits of Tiran and near 28°N between the Gulf of Suez and the Red Sea. A better understanding of the hydrographic structure of the Red Sea can be obtained through seasonal measurements of temperature and salinity at locations more evenly distributed within the basin than data used in this study. These observations should be taken along and perpendicular to the central axis. Additionally, measurements of other parameters (nutrients and dissolved oxygen, for example) will provide sufficient information to allow expansion of the water mass analysis into three- or four-space rather than the present two-space of temperature and salinity. This expansion would reduce the ambiguity of the present method when more than three parent water types are used. The resulting comprehensive data sets would provide sufficient information to determine formation regions, and budgeting of Red Sea water types and water masses.

BIBLIOGRAPHY

Biblik, V. A. Investigation of the Red Sea tides. In: The Ocean World, M. Uda (ed.) Japan Society for the Promotion of Science, Tokyo, p. 57-66, 1971.

Boisvert, W. E. Ocean currents in the Arabian Sea and northeast Indian Ocean. Naval Oceanogr. Office Rep. SP-92, 1966.

Defant, A. Physical Oceanography, Vol. I, The MacMillan Company, New York, 729 p., 1961.

Dubrovin, B. I. Volumetric statistical analysis of the water masses in the Arabian and Red Seas. Okeanologiya, V, v. 4. p. 52-55, 1965.

Eugene, L. B. Handbook of Oceanographic Tables. Naval Oceanographic Office, Rep. SP-68, 1966.

Everett, N. J. and David G. Browning. Cold layer in the southern Red Sea, Limnol. & Oceanogr., Vol. 16, No. 3, p.503-509, 1971.

Flohn, H. Local wind systems. In: World survey of climatology, Vol. 2, H. E. Landsberg (gen. ed.). Elsevier Publishing Company, New York, p. 124-144, 1969.

Koninnklijk Nederlands Meteorologisch Institute. Red Sea and Gulf of Aden Oceanographic and Meteorological Data. Publ. 120, 26 p., 1949.

Maillard, G. Etude hydroloique et dynamique de la Mer Rouge en hiver le observations du COMMANDANT ROBERT GIRAUD (1963). These présentée a La Faculte Des Sciences De Paris pour L'obtention du Doctorat 3e cycle, 77 p, 1971.

Monin, A. S. and E. A. Plakhin. Stratification and space time variability of Red Sea hot brines. Deep Sea Res. 29, No. 11A, 1982.

Morcos, S. A. Physical and chemical oceanography of the Red Sea. Oceanogr. Mar. Biol. Ann. Rev., 8, p. 73-202, 1970.

Neumann, A. C. and D. A. McGill. Circulation of the Red Sea in early summer. Deep Sea Res., 8, 223-235, 1961.

Patzert, W. C. Seasonal variations in structure and circulation in the Red Sea, Ph.D. thesis, Hawaii Institute of Geophysics, University of Hawaii, 58 p., 1972.

Privett, D. W. Monthly charts of evaporation from the N. Indian Ocean including the Red Sea and the Persian Gulf. Quart. J. Roy. Meteorol. Soc., 85, 424, 1959.

Rosenblum, L. J. Real time applications software for the Neil Brown/ W.H.O.I. CTD Microprofiler. Naval Research Laboratory NRL Rep. 844, 43 p., 1980.

Ruzecki, E. P. On the water masses of Norfolk Canyon. Ph.D. thesis, University of Virginia, 293 p., 1979.

Siedler, G. Schichtungs-und Bewegungsverhältnisse am Sudansgan des Rotem Meers. Meteor. Forschungserbuise Reihe A, No. 4, 76 p., 1968.

Siedler, G. General circulation of water masses in the Red Sea. In: Hot brines and recent heavy metal deposits in the Red Sea. E. T. Degens and D. A. Ross (ed.), Springer-Verlag, New York, Inc., p. 131-137, 1969.

Sokal, R. R. and F. J. Rohlf. Biometry. W. H. Freeman and Company, San Francisco, p. 148-162, 1969.

Sverdrup, H. U., M. W. Johnson and R. H. Fleming. The Oceans, Their Physics, Chemistry and General Biology. Prentice-Hall, Inc., p. 137-150, 1942.

Thompson, E. F. Chemical and physical investigations. The general hydrography of the Red Sea. John Murray Exped. 1933-34, Sci. Rep. 2(3), p. 83-103, 1939a.

Thompson, E. F. Chemical and physical investigations. The exchange of water between the Red Sea and the Gulf of Aden over the 'sill'. John Murray Exped. 1933-34, Sci. Rep. 2(4); p. 105-119, 1939b.

Wright, W. R. and C. E. Parker. Avolumetric temperature/salinity census for the Middle Atlantic Bight. Limnol. & Oceanogr. 21(4):563-571, 1976.

Yegorov, N. I. Calculation of the heat balance of the Red Sea. Meteorologiia i Gidrologiia No. 3, p. 49-56, 1950. (in Russian)

VITA

Mohamed Zaki Moustafa

Born in Ismailia, Egypt, August 31, 1951. Attended Maadi School (1957-1966) and Maadi High School (1966-1969) in Cairo, Egypt. Obtained a Bachelor Degree in Naval Studies from Egyptian Naval Academy, Alexandria, Egypt, 1973. Obtained a diploma in hydrographic and oceanographic survey from Naval Oceanographic Office, Bay St. Louis, Mississippi, 1980. Entered the master program at the School of Marine Science, College of William and Mary in 1980.